Marine Pollution Bulletin 221 (2025) 118495

Contents lists available at ScienceDirect

Marine Pollution Bulletin

journal homepage: www.elsevier.com/locate/marpolbul

Comparing persistent (polycyclic aromatic hydrocarbons and polychlorinated biphenyls) and emerging nano(micro)plastics (NMPs) pollutant body-burdens in oysters and fish from Matagorda Bay (Texas, USA)

Asif Mortuza [a,*], Emily N. Meese [a], Marcus Wharton [b], Bryan Gahn [b], Lene H. Petersen [a], Antonietta Quigg [a,c,d], R.J. David Wells [a,d], Karl Kaiser [b], David Hala [a,d]

[a] Department of Marine Biology, Texas A&M University at Galveston, Galveston, TX 77553, USA
[b] Department of Marine and Coastal Environmental Science, Texas A&M University at Galveston, Galveston, TX 77553, USA
[c] Department of Oceanography, Texas A&M University, 3146 TAMU, College Station, TX 77843, USA
[d] Department of Ecology and Conservation Biology, Texas A&M University, 3146 TAMU, College Station, TX 77843, USA

ARTICLE INFO

Keywords:
Coastal estuary
Shellfish
Fish
Microplastics
Body-burdens
Risk assessment

ABSTRACT

This study reports the concentrations of 12 nano (micro)plastics (NMPs, ≥700 nm particle size, <5 mm), 14 polycyclic aromatic hydrocarbons (PAHs), and 28 polychlorinated biphenyls (11 dioxin-like PCBs) in the gill/mantle tissue of eastern oysters (*Crassostria virginica*) and muscle and liver tissues of gafftopsail catfish (*Bagre marinus*), red drum (*Sciaenops ocellatus*), and spotted sea trout (*Cynoscion nebulosus*) from Matagorda Bay (Texas, USA). Pyrolysis gas chromatography and tandem mass spectrometry (Py-GCMS/MS) was used to quantify the NMPs, and GCMS was used for PAHs and PCBs quantification. Analysis of the total contaminant concentrations across all the biota showed NMPs to exhibit the highest body-burdens (~2000×–201360,000×) relative to PAHs and PCBs. Amongst the biota, oysters exhibited the highest contaminant body-burdens in comparison to fish. For PAHs and PCBs, the gill/mantle of oysters exhibited ~2–11× higher body-burdens than the muscle tissue of fish and NMPs in oysters were 5–25× higher (body-burdens) than in fish muscle. Diagnostic ratio analysis revealed a mixture of both petrogenic and pyrogenic sources of PAHs. Toxic equivalent (TEQ) based risk assessment for dioxin-like PCBs indicated the likelihood for adverse health effects in gafftopsail catfish only. A cancer risk assessment for human exposure to PAHs from seafood consumption showed no concern. Finally, the calculation of human average daily NMPs consumption indicated the ingestion of 0.01–0.2 g plastics/kg of body weight/year. A key finding of our work is that the body-burdens of NMPs were several orders of magnitude higher than those for PAHs and PCBs.

1. Introduction

The U.S. coastline along the northern Gulf of Mexico is a heavily developed coastal zone with an extensive urban and industrial zone, ~10 % higher than the national average (census.gov, 2019; comptroller.texas.gov, 2020). Furthermore, its offshore zone hosts ~3200 active oil and gas structures (NOAA, 2024). Such a high level of development has led to concerns for aquatic pollution from persistent pollutants, such as oil or combustion derived polycyclic aromatic hydrocarbons (PAHs), and 'legacy' pollutants such as polychlorinated biphenyls (PCBs) (Frank et al., 2001; Kennicutt, 2017; Oziolor et al., 2018; Pulster et al., 2020; Rowe et al., 2020). However, there is recent concern for the presence of so-called 'emerging' pollutants, such as pharmaceuticals, per/poly-fluoroalkyl substances (PFAS), and microplastics (<5 mm) in near-shore coastal environments (Arman et al., 2021; Deblonde et al., 2011; Gavrilescu et al., 2015; Geissen et al., 2015). Given these concerns, there is an overall paucity of information on the presence of emerging pollutants (especially microplastics) in the aquatic environment (Bhattacharya and Khare, 2022; Burns and Boxall, 2018; Horton et al., 2017; Mintenig et al., 2018).

In this manuscript we quantified the body-burdens of select PAHs, PCBs, and nano(micro)plastics (NMPs) in the biota (oysters and fish) of a

* Corresponding author.
E-mail address: morta02@tamu.edu (A. Mortuza).

https://doi.org/10.1016/j.marpolbul.2025.118495
Received 9 April 2025; Received in revised form 11 June 2025; Accepted 22 July 2025
Available online 28 July 2025
0025-326X/© 2025 The Authors. Published by Elsevier Ltd. This is an open access article under the CC BY license (http://creativecommons.org/licenses/by/4.0/).

northwestern Gulf of Mexico estuary, Matagorda Bay. Located along the upper mid coast of Texas, it is the second largest estuary in Texas (TSHA, 2023) (Fig. 1). On average, the bay is 2 m deep and occupies an area of 1093 km^2 with a long hydraulic residence time of 237 days (TSHA, 2023). Matagorda Bay receives discharge from major riverine sources such as the Lavaca and Colorado rivers (TSHA, 2023). The natural wildlife of Matagorda Bay serves the local birding and fishing tourism industry, with commercial fishing generating $7.8 million dollars in revenue annually (Robinson et al., 1996). The bay is also home to major chemical industries such as the Aluminum Company of America, Union Carbide, Du Pont, and Formosa Plastics (TSHA, 2023). It is also home to the South Texas Nuclear Generating Station in nearby Bay City (TSHA, 2023). Recently, the Formosa Plastics company (Point comfort, Matagorda Bay near sampling site A, Fig. 1) was litigated against and found liable for the release of plastic nurdles (i.e., plastic pellets) into the bay (Anchondo, 2019; Conkle, 2018). The case was settled for a fine of $50 million dollars to Formosa Plastics (Conkle, 2018; Moore-Eissenberg, 2019).

This study provides for a comprehensive analysis, a snapshot in the state of legacy (PAHs and PCBs) and emerging (NMP) pollutant body burden in the biota (fish and oyster) of Matagorda Bay, a bay system with both industrial and commercial fishing activities. In doing so, we have used a well-established gas chromatography and mass spectrometry (GCMS) method to measure the levels of 14 EPA priority PAHs and 28 PCBs (including 11 dioxin-like PCBs or DL-PCBs) in oysters (gill/mantle) and fish (liver and muscle). And a novel pyrolysis gas chromatography and tandem mass spectrometry (Py-GCMS/MS) method was established and used to comprehensively quantify 12 common NMPs in the biota. We hypothesized that the legacy and lipophilic nature of PAHs and PCBs pollutants will result in their greater body-burdens in biota relative to NMPs (which are considered as emerging pollutants). In addition, to measuring the body-burdens of pollutants, the likely sources of PAHs in the bay were assessed by comparing the ratios of diagnostic low to high molecular weight (LMW vs. HMW) PAHs (Tobiszewski and Namieśnik, 2012). The cancer risk of PAHs to the human consumers of seafood was calculated, and a toxic equivalents (TEQs) risk assessment was performed to determine likely adverse health effects of the dioxin-like PCBs (DL-PCBs) in fish (Barron et al., 2004; Van den Berg et al., 1998). Lastly, the adult human average yearly intake of plastics from seafood was evaluated using the NMPs levels measured in the gill/mantle of oysters and the muscle tissue of fish (Nolen et al., 2022).

2. Methods

2.1. Sample collection and preparation

The following biota were sampled from Matagorda Bay due to their abundance and economic value: eastern oysters (*Crassostria virginica*, Gmelin, 1791), gafftopsail catfish (*Bagre marinus*, Mitchill, 1815) (hereafter catfish), red drum (*Sciaenops ocellatus*, Linnaeus, 1776), and spotted sea trout (*Cynoscion nebulosus*, Cuvier, 1830) (Dailey, 1977;

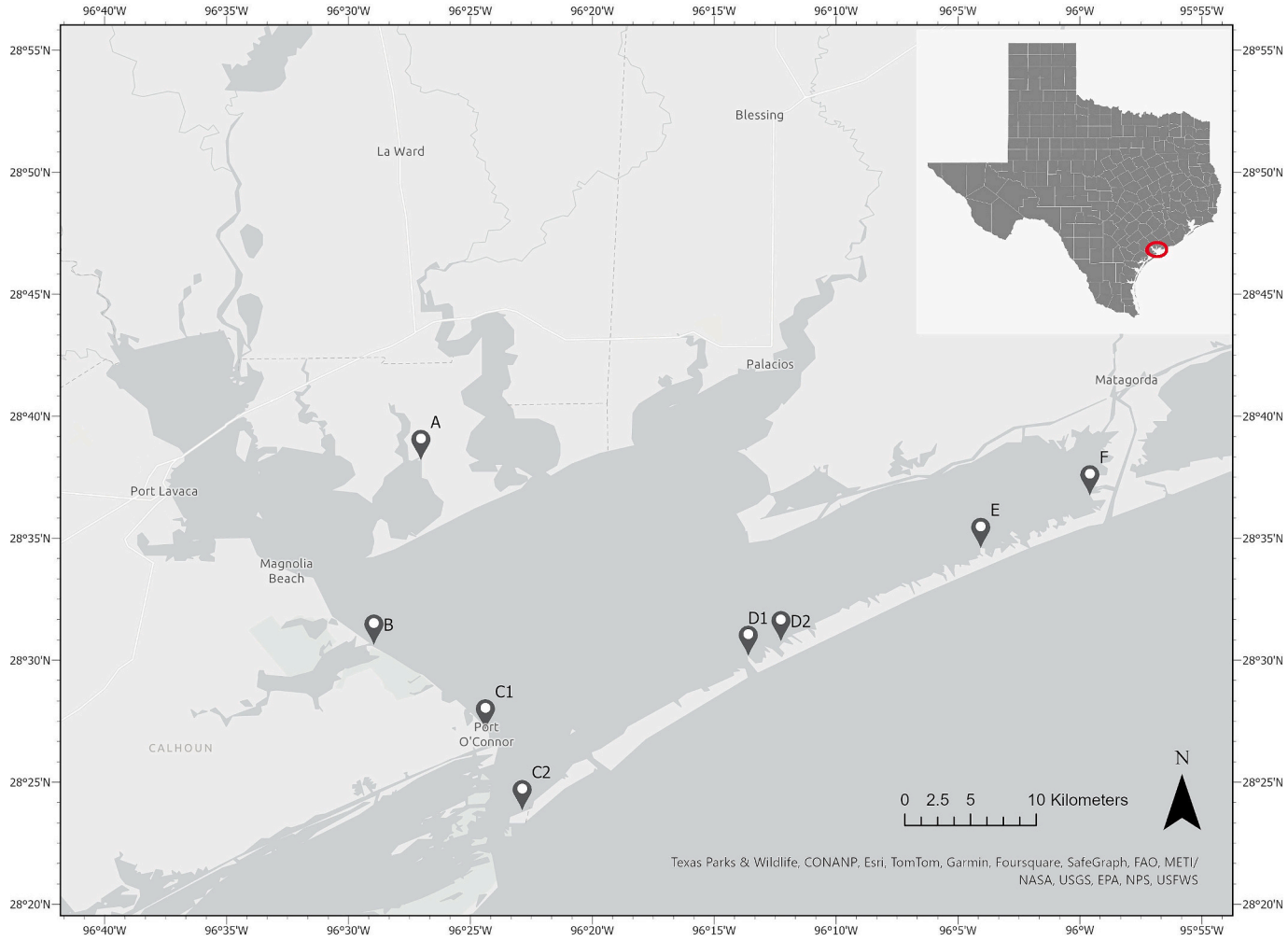

Fig. 1. A map of Matagorda Bay showing its location along the Texas coastline (inset map) located in the northwestern Gulf of Mexico. Fish and oysters were sampled at various locations around the bay.

Ropicki et al., 2016; Vega et al., 2011). The oysters are useful for their filtering capacity (Ehrich and Harris, 2015; NOAA, 2020) as well as a widely studied sentinel species (Cantillo, 1997; Goldberg et al., 1978). The fish and oysters were caught using a variety of catch methods such as benthic sled tows, bag seines, gill nets, and entanglement nets. All oysters and fish were weighed, and their total length (TL) and fork length (FL) (fish only) measured (Supplemental Table 1). Similar size specimens were used from each species. After sampling from the bay, the fish were euthanized with cervical dislocation and put on ice, and transported to the lab, where a skin-free muscle fillet and liver biopsy were excised from each fish, and gill/mantle tissue was collected from each oyster. All tissue samples were stored at −20 °C until analysis. Prior to analysis, ~0.5 g of frozen tissue was lyophilized for 24 h at 0.20 mBar vacuum and −87 °C using a LABCONCO freeze dryer. The resulting freeze-dried tissue was pulverized into a fine powder using a pestle and mortar.

2.2. PAH and PCB quantification

An accelerated solvent extraction (ASE) system (Dionex ASE 350) was used to extract PAHs and PCBs. Approximately 0.5 g of previously freeze-dried, pulverized, muscle or liver tissue was packed into a 34 mL stainless steel ASE cell, with the remainder volume packed with Ottawa sand (standard 20–30 mesh, Cat# S1010, Spectrum Chemical) above and below the sample. The sample was spiked with 10 μL of 50 μg/mL internal standards B[*a*]P-d_{12} and PCB65-d_5. Control or blank cells (comprising Ottawa sand only) were also spiked with internal standards to account for any background contamination. Solvent extraction was conducted at 100 °C and 1500 psi pressure with a heating time of 5 min, preheat 5 min and a static phase of 4 min in the ASE. The flush rate was 60 % with a purge time of 300 s. Two static cycles were completed per sample. The resulting solvent extracts were collected in 50 mL amber glass bottles and dried under a gentle stream of nitrogen (N_2). The resulting residue was reconstituted in 1 mL dichloromethane (ThermoFisher) and transferred to a smaller 5 mL test tube. The resultant solution was then subjected to solid phase extraction through a Captiva lipid filter cartridge (Agilent Captiva EMR- Lipid, 1 mL, 40 mg) using a vacuum manifold to remove lipids from the sample. Each solid phase extraction cartridge was conditioned with 1 mL dichloromethane, followed by the entire sample volume passing through the cartridge at a steady rate of ~1 drop/s. The recovered solution was dried under a gentle stream of N_2, with the resulting residue reconstituted into 0.2 mL acetonitrile. The resuspended solution was transferred to a small volume glass insert and frozen at −20 °C to promote the precipitation of any remainder lipids and tissue debris (Hong et al., 2004). Subsequently, 0.1 mL of the solvent supernatant was removed and dried under N_2, with the final residue reconstituted into 0.1 mL dichloromethane, pipetted into a small volume insert and analyzed via GCMS.

The concentrations of PAHs and PCB congeners were quantified using GCMS: acenaphthene (ACE), fluorene (FLU), anthracene (ANT), phenanthrene (PHE), fluoranthene (FLT), chrysene (CHR), pyrene (PYR), benzo [a] anthracene (BaA), benzo [b] fluoranthene (BbF), benzo [k] fluoranthene (BkF), benzo [a] pyrene (BaP), dibenz [a,h] anthracene (DahA), benzo [g,h,i] perylene (BghiP), and indeno [1,2,3-cd] pyrene (IcdP). The 28 PCB congeners include PCBs 1, 18, 33, 52, 77, 81, 95, 101, 105, 114, 118, 123, 126, 128, 138, 149, 153, 156, 157, 167, 169, 170, 171, 177, 180, 183, 187, and 189. All PCBs are identified according to the IUPAC numbering system. EPA priority pollutant PAHs were picked along with various DL-PCBs due to their toxicity. The GCMS analysis was performed using a Hewlett Packard HP 6890 Series GC System coupled with Agilent Technologies 5973 Mass Selective Detector. Samples were injected in splitless mode (2 μL) onto a DB-5MS (J&W Scientific) capillary column (30 m × 0.25 mm i.d.: 0.25 μm film thickness). Helium was used as the carrier gas at a flow rate of 1.0 mL/min. Temperatures at the front inlet and the MS interface were set to 250 °C and 280 °C, respectively. Following the injection of the sample, the GC oven initiated at 40 °C for 1 min, then ramped up to 180 °C at 20 °C/min, and then to 300 °C at 5 °C/min, for a hold of 10 min. The total runtime of the method was 40 min. The MS was operated in electron impact (EI) mode at an electron energy of 70 eV, while the MS source temperature was maintained at 230 °C. Selected ion monitoring mode was used to identify and quantify all 42 analytes. The respective retention times for the PAHs and associated $^{m}/_{z}$ ions selected for quantification are reported in Hernout et al. (2020). The quantification of each PAH and PCB was performed against a linear 11-point calibration curve using serially diluted standards from 10 to 0.01 μg/mL. The limit of detection (LOD) for each compound was determined as the lowest standard that yielded a signal-to-noise ratio ≥ 5:1. Therefore, any analyte giving a response 5× above the background was considered an appropriate (quantifiable) signal. All body-burden concentrations are reported as ng/g tissue dry weight (or ng/g DW).

Sample quality assurance included the preparation of sample blanks comprising Ottawa sand spiked with internal standards. Blanks yielding values for a compound greater than the respective limit of detection was used for background correction by subtracting its averaged value from all samples. Standard addition samples were also spiked with select PAHs (BaA and PYR) and PCBs (PCB 18 and 101) into muscle and liver from fish to measure recovery. For every batch of ten muscle or liver samples analyzed, two additional blanks and a standard addition sample were included for quality assurance. The average recovery of selected PAHs and PCBs was (mean ± s.e.m), 74.07 ± 0.44 % for BaA, 46.01 ± 9.24 % for PYR, 69.07 ± 3.88 % for PCB 18, and 68.5 ± 5.83 % for PCB 101.

2.3. Source assessment of PAHs

To identify the predominant sources of PAHs, diagnostic source ratios of various HMW to LMW PAHs were compared. HMW PAHs comprise ≥4 aromatic rings are typically products of combustion at higher temperatures (400–700 °C) and are therefore mainly pyrogenic in origin. Whereas LMW PAHs comprise <4 aromatic rings and are products of combustion at lower temperatures (i.e., 100–300 °C), and are therefore considered to be mainly petrogenic in origin (Budzinski et al., 1997; Wolska et al., 2012). Diagnostic ratios of ∑LMW/∑HMW, ∑COMB (all HMW PAHs)/∑PAH (i.e. LMW + HMW), FLT/(FLT + PYR), ANT/(ANT+PHE), BaA/(BaA + CHR), IcdP/(IcdP+BghiP), BaP/BghiP, and PHE/ANT were used to help identify PAH sources and are detailed Table 3 (Tobiszewski and Namieśnik, 2012).

2.4. Cancer risk assessment of PAHs

To evaluate the cancer risk via sea food consumption, a BaP equivalent (BaPE) concentration for fish body-burdens was calculated and compared against the Level of Concern concentration calculated by the FDA risk assessment for exposure risk from the consumption of fish (0.035 μg/g BaPE) or oysters (0.142 μg/g BaPE) (FDA, 2010). In addition to considering the BaP body-burdens to calculate the BaPE, the individual toxicity equivalent factors (or TEFs) for PAHs whose toxicity have been standardized to that of BaP (i.e., BaA, CHR, BbF, IcdP, and DahA) were also summed to that of the BaPE value to generate an overall concentration for comparison with the FDA reference values for fish and oysters. BaPE concentration was reported in μg/g of wet weight (WW)

BaPE. Only muscle tissue body-burden was calculated as it is the component consumed by humans. The formula used is as follows:

$$\text{BaPE concentration} = \text{BaP cocentration} + \sum(\text{equivalent PAHs concentration x respective TEFs})$$

2.5. Toxicity equivalents assessment of dioxin-like PCBs (or DL-PCBs)

To assess the potential toxicity of DL-PCBs to fish, toxic equivalents (TEQs) were calculated using toxic equivalent factors (TEFs) as proposed by Van den Berg et al. (1998). This approach takes into account the additive effects of DL- PCBs (i.e., non-ortho and mono-ortho PCBs) congeners in hepatic tissue. The toxicity potential was assessed for eleven DL-PCBs quantified in fish livers, namely PCBs 77, 81, 105, 114, 118, 123, 126, 156, 167, 169, and 189. The remainder PCBs were non-dioxin-like or NDL-PCBs. The lipid-normalized hepatic body-burden of each congener was multiplied with its respective TEF, and then summed to calculate the TEQ value (Van den Berg et al., 1998). The summed TEQ values for each fish species were reported as $\log_{10}$ pg/g lipid weight (LW) and compared against reported upper and lower limit values shown to be toxic in aquatic mammals (1400–160 pg/g LW) and fish (600–57 pg/g LW) (Kannan et al., 2000; Steevens et al., 2005). Steevens et al. (2005) determined the TEQ upper and lower limits that were protective (survival) of 90 % and 99 % of fish respectively, whereas Kannan et al. (2000) determined high TEQ values that are associative with immunosuppression and endocrine disruption in marine mammals.

2.6. Nano(micro)plastics (NMPs) quantification

An enzyme solution was prepared to digest the freeze dried tissue samples for NMP extraction using a protocol adapted from von Friesen et al. (2019). Briefly, 6 g of porcine pancreatic enzyme (Pez, Millipore-Sigma, CAS# 8049-47-6) was dissolved into 100 mL of tris (tris (hydroxymethyl) aminomethane)/tris hydrochloride solution (Sigma-Aldrich, Cat# T3038). Pez contains protease, amylase, and lipase enzymes, which help break down proteins and lipids in the tissue to release microplastics particles from the tissue matrix. To further remove any plastics contamination from the pancreatic enzyme, the Pez/Tris solution was placed in an oven at 40 °C for 3 h and then vacuum filtered through 2.8 μm and 0.7 μm glass fiber filters (CYTIVIA Whatman GF/F and GF/D, VWR) using a Brinkmann Model B-169 vacuum aspirator. Approximately 0.02 g of dried fish and oyster tissue was placed in round bottom glass vials to be treated with 1 mL of Pez/Tris solution (0.06 g Pez/mL buffer) while maintaining an optimal pH 8 for pancreatic enzymes (Berdutina et al., 2000). The vials were then shaken for 24 h at 40 °C on a shaker tray. The samples were then filtered through cleaned and furnaced 0.7 μm × 24 mm glass fiber filters using a vacuum filter and rinsed with Milli-Q water (Milli-Q EQ. 7000 Ultrapure Water Purification System, Merck KGaA, Darmstadt, Germany). The utilized portion of each filter was then cut out using a cork borer, separated and placed in a glass Petri dish where it was dried for 24 h at 38 °C. The filters were folded after drying and placed in separate stainless-steel Pyrolysis cups (Eco-Cup LF, Frontier Labs, Japan) that had been treated with 20 μg of polyfluorinated styrene as internal standard. Finally, the sample cups were topped with 5 mg of calcium carbonate and quartz wool to pack the sample and placed in a Frontier Laboratories Ltd. Auto-Shot Sampler: AS-1020E Pyrolizer for pyrolysis GCMS analysis.

A Frontier Laboratories Auto-shot sampler pyrolyzer in conjunction with an Agilent 8890 GC System coupled with an Agilent 7010B triple quadrupole mass spectrometer (Py-GCMS/MS), was used to identify and quantify plastics polymers. The microplastics quantified included all common consumer use plastics such as: polymethyl methacrylate (PMMA), polypropylene (PP), polyvinyl Chloride (PVC), polyamide (PA), polycarbonate (PC), nylon 66 (N66), polyethylene (PE), polyethylene terephthalate (PET), acrylonitrile butadiene styrene (ABS), polyurethane (PUR), styrene-butadiene rubber (SBR), and polystyrene (PS). The pyrolysis or combustion of tissue samples at 600 °C allowed for the complete oxidation of organics, while the microparticles were volatilized and fragmented to smaller and more stable particles (pyrolyzates). These pyrolyzates were chromatographically separated using an Ultra Alloy^{+}-5 Capillary Column (30 m length x 0.25 mm I.D. x 0.25 μm film) (Frontier Labs, Japan) in an Agilent 8890 GC System with an increasing temperature gradient before being introduced to an Agilent 7010B GCMS/MS Triple Quadrupole for precise mass analysis. The injector was set to a split ratio of 50:1, with a split flow of 40 mL/min. The injector temperature was set to 300 °C. The septum purge flow was 20 mL/min. Straight liners packed with non-deactivated glass wool were used. Helium at a flow rate of 2.25 mL/min was used as the carrier gas and nitrogen at 1.5 mL/min was used as the collision gas. Chromatographic separation was achieved with the following temperature program: starting temperature 35 °C, hold for 0.25 min, ramp at 20 °C/min to 310 °C, hold for 3 min, a total runtime of 17 min. The mass detector settings were: source temperature 230 °C, quad temperature 150 °C, and auxiliary temperature 280 °C, with a 5 min solvent delay. MassHunter acquisition and associated data analysis software were used for accurate mass analysis. The quantification of individual plastic polymers was based on individual distinctive mass ions (Supplemental Table 3). The quantification of each polymer was performed against a linear five-point calibration curve spanning from 1500 to 150 μg, with 40 μg of Internal standard (polyfluorinated styrene, PFS). All standards were placed onto a GF/F (0.7 μm pore size, 25 mm diameter) Whatman filter, transferred into Eco-cups (Frontier Labs, Japan), packed with 5 mg of $CaCO_3$, and finally sealed with quartz wool. LODs were calculated using a Signal/Noise threshold of $\geq$3.

To correct for the interference of lipids on polyethylene quantification as described by Rauert et al. (2022), we used a lipid triglyceride mixture from Sigma (CAS# 17810) as control. We found sample lipids to mainly interfere with the quantification of PE, PP, N66, PMMA, and PVC. To account for lipid contamination, a 5-point lipid calibration curve was constructed from 0.25 mg to 1.25 mg using the weights of lipids against the concentration for each of the plastics. Assuming, there were no plastics in the lipid standard from Sigma, this calibration curve showed the relation between lipid concentrations and lipid content, therefore yielding a correction factor which was subtracted from the plastic quantification in each sample.

For each batch of 10 samples, two blank controls, two recovery controls, and a replicate were also analyzed. Each blank control pyrolysis cup contained 40 μg of Internal standard (Polyfluorinated styrene), GF/F (0.7 μm pore, 25 mm diameter), Whatman filter (after filtering 1 mL of Pez/Tris), 5 mg of $CaCO_3$, and quartz wool to measure background contamination to be subtracted from sample quantification. The standard addition/recovery control contained 40 μg of Internal Standard (Polyfluorinated styrene), GF/F Whatman filter (0.7 μm) containing a known amount of the Frontier plastics standard (Frontier labs, Lot# 21101501), 0.02 g of dry weight tissue (digested with 1 mL of Pez/Tris), 5 mg of $CaCO_3$, and quartz wool to measure the percentage recovery of plastic standards. The replicate pyrolysis cups also contained a replicate of a sample (muscle matrix) to confirm reproducibility of data. The percent recovery of notable plastics in the muscle matrix was 115 ±

0.15 % for PP, 93 ± 0.08 % for N66, and 113 ± 0.05 % for PE.

2.7. Estimated average daily intake of plastics

Seafood Daily Intake (DI) and NMPs Average Daily Intake (ADI) rates were calculated as follows:

$$DI = \frac{DC_{shellfish\ or\ fish}}{BW} \quad (1)$$

$$ADI = C_{Plastics} \times DI \quad (2)$$

First, a seafood daily intake (DI) in g/kg human body weight/day was determined by dividing the estimated daily consumption ($DC_{shellfish/fish}$) of shellfish or fish (in g/day) by the body weight (BW) of an average adult human (kg) (Eq. (1)). The Texas Department of State Health Services' Seafood and Aquatic Life Group's standard adult weight of 70 kg and consumption of 30 g of shellfish or fish per day were used to calculate the DI (DSHS, 2011). Subsequently, an Average Daily Intake (ADI) rate of plastics consumption (in mg/kg human body weight/day) was calculated by multiplying the average plastics concentration in muscle of fish or gill/mantle of oysters in μg/g wet weight ($C_{plastics}$) by the DI (Eq. (2)). While the $C_{plastics}$ were initially quantified as μg/g dry weight (DW), the DW values were converted to their respective wet weight (WW) basis by using an average correction factor (for each species) that accounted for the proportion of tissue weight change after freeze-drying, i.e., indicating the loss of tissue water content (see above). Finally, the ADI in mg/kg human body weight/day was converted to an annual or yearly plastics intake by multiplying the ADI's for each species by 365 days.

2.8. Statistical analysis

Statistical analysis was conducted using R (v 4.1.3) with significance at $p \leq 0.05$ (R, 2024). The normality of data was tested using Shapiro-Wilk's test followed by Levene's test for homogeneity of variance. For pairwise comparisons, either a parametric *t*-test or non-parametric Mann-Whitney *U* test was conducted. The statistical analysis of data comprising a main effects variable was performed using either one-way ANOVA (parametric) or the Kruskal-Wallis test (non-parametric), with post hoc testing comprising either Tukey's or Dunn's test respectively.

3. Results

3.1. Morphometric parameters

Amongst the fish species sampled, gafftopsail catfish and spotted sea trout were within the adult size range, whereas red drum were categorized as juveniles as shown in Supplemental Table 1. A spearman-rank correlational analysis was conducted between morphometric parameters and the pollutant body-burdens, with no significant correlations reported (data not shown).

3.2. Persistent pollutant body-burdens in biota

The sum of total (Σ) PAH levels in fish muscle showed no significant differences ($p \leq 0.05$) across the biota (Table 1(a)). Oysters, however, exhibited the highest (not significant) concentrations at levels 2× higher than those in catfish, and 1.2× of sea trout and red drum respectively (Table 1(a)). Fish livers exhibited ΣPAH levels 5×–14× higher than those measured in the muscle tissue (Table 2(a)), with a significant difference only between red drum and catfish being evident (levels 4× higher in red drum).

A comparison of PAH congener profiles showed a broad representation of LMW and HMW PAHs in fish muscle compared to liver (Supplemental Figs. 1 and 2). In the muscle of fish (and gill/mantle of oysters), PHE levels equivalently dominated in all species with levels

Table 1
Oysters (gill/mantle tissue) and fish muscle concentrations of a) PAHs, b) PCBs, and c) NMPs. Levels are reported in ng/g DW for PAHs and PCBs, and μg/g DW for NMPs (mean ± standard error). Levels below the limit of detection are represented by '-'. Different letters for sum of total show significant differences ($p \leq 0.05$) between species.

	Oysters (n = 10)	Catfish (n = 10)	Red drum (n = 7)	Sea trout (n = 9)
a) PAHs (ng/g DW)				
Low molecular weight (LMW)				
Acenaphthene (ACE)	17.79 ± 5.73	12.27 ± 2.46	6.47 ± 0.71	15.80 ± 3.01
Fluorene (FLU)	19.53 ± 11.17	8.97 ± 1.43	1.83 ± 1.25	8.30 ± 4.01
Phenanthrene (PHE)	28.50 ± 8.32	23.10 ± 5.24	11.55 ± 1.07	44.91 ± 20.74
Anthracene (ANT)	1.31 ± 0.50	14.36 ± 3.23	3.83 ± 1.41	8.12 ± 3.13
High molecular weight (HMW)				
Fluoranthene (FLT)	4.48 ± 2.54	28.02 ± 5.14	2.22 ± 2.22	9.59 ± 5.75
Pyrene (PYR)	8.47 ± 2.60	31.13 ± 5.18	6.57 ± 1.73	22.71 ± 3.62
Benzo[*a*] anthracene (BaA)	114.48 ± 40.45	2.80 ± 1.87	114.71 ± 59.47	30.95 ± 16.33
Chrysene (CHR)	15.72 ± 3.15	0.91 ± 0.61	19.06 ± 15.24	13.06 ± 9.44
Benzo[*b*] fluoranthene (BbF)	-	-	3.44 ± 1.27	7.30 ± 1.83
Benzo[*k*] fluoranthene (BkF)	1.13 ± 0.95	0.25 ± 0.25	1.80 ± 1.21	8.90 ± 1.71
Benzo[*a*]pyrene (BaP)	4.62 ± 2.37	-	1.43 ± 0.93	2.82 ± 2.12
Indeno[1,2,3-*cd*] pyrene (IcdP)	2.96 ± 1.29	-	22.72 ± 1.89	20.23 ± 2.28
Dibenzo[*a*,*h*] anthracene (DahA)	6.21 ± 2.20	2.59 ± 0.80	2.48 ± 0.88	2.60 ± 1.48
Benzo[*g*,*h*,*i*] perylene (BghiP)	5.31 ± 1.25	-	0.80 ± 0.80	1.12 ± 0.75
ΣPAHs	**230.50 ± 82.53[a]**	**124.40 ± 26.21[a]**	**198.91 ± 90.08[a]**	**196.40 ± 76.18[a]**
b) PCBs (ng/g DW)				
Non-ortho (dioxin like)				
PCB 77	62.08 ± 33.90	1.00 ± 1.00	4.09 ± 3.19	-
PCB 81	17.07 ± 9.83	1.30 ± 0.67	7.30 ± 4.11	-
PCB 126	1.01 ± 1.01	12.84 ± 8.87	2.76 ± 2.23	0.57 ± 0.38
PCB 169	-	0.99 ± 0.32	0.68 ± 0.68	2.21 ± 1.14
Mono-ortho (dioxin like)				
PCB 105	3.16 ± 1.44	3.50 ± 1.92	6.02 ± 1.98	7.41 ± 4.29
PCB 114	26.83 ± 12.80	1.17 ± 0.82	3.82 ± 2.08	1.97 ± 1.00
PCB 118	4.71 ± 1.89	0.70 ± 0.70	5.74 ± 4.02	1.66 ± 0.85
PCB 123	3.60 ± 1.22	0.84 ± 0.84	2.40 ± 1.84	1.61 ± 0.82
PCB 156	5.92 ± 2.01	-	11.54 ± 7.48	1.11 ± 1.11
PCB 167	2.70 ± 1.50	-	-	4.62 ± 4.62
PCB 189	0.29 ± 0.29	-	-	-
Non-dioxin like				
PCB 1	4.70 ± 1.78	-	-	-
PCB 18	109.24 ± 29.54	2.34 ± 1.45	86.44 ± 54.78	31.12 ± 14.61
PCB 33	36.62 ± 12.17	0.48 ± 0.48	6.58 ± 3.83	0.79 ± 0.79

(*continued on next page*)

Table 1 (*continued*)

	Oysters (n = 10)	Catfish (n = 10)	Red drum (n = 7)	Sea trout (n = 9)
PCB 52	0.31 ± 0.31	-	1.25 ± 0.59	0.21 ± 0.17
PCB 95	1.22 ± 0.82	-	1.33 ± 0.86	-
PCB 101	2.99 ± 1.21	-	1.99 ± 1.99	-
PCB 128	1.89 ± 1.25	1.09 ± 0.73	0.57 ± 0.57	7.94 ± 7.94
PCB 138	0.93 ± 0.49	-	-	0.45 ± 0.45
PCB 149	0.87 ± 0.46	-	4.42 ± 3.12	-
PCB 153	0.32 ± 0.22	-	0.65 ± 0.65	0.77 ± 0.77
PCB 157	0.85 ± 0.46	-	2.49 ± 1.63	-
PCB 170	0.30 ± 0.30	-	1.32 ± 1.32	0.60 ± 0.60
PCB 171	0.76 ± 0.76	-	3.69 ± 1.95	-
PCB 177	-	-	3.44 ± 2.23	0.49 ± 0.49
PCB 180	1.00 ± 0.52	-	-	-
PCB 183	0.37 ± 0.37	-	-	-
PCB 187	0.55 ± 0.55	-	-	0.51 ± 0.51
ΣPCBs	**290.29 ± 117.10[a]**	**26.25 ± 17.80[b]**	**158.53 ± 101.14[ab]**	**64.04 ± 40.53[ab]**
c) NMPs (μg/g DW)				
Polymethyl methacrylate (PMMA)	-	-	-	-
Polypropylene (PP)	5320.77 ± 2442.74	-	-	-
Polyvinyl Chloride (PVC)	-	-	-	-
Polyamide (PA)	-	-	-	33.66 ± 18.05
Polycarbonate (PC)	-	-	-	-
Nylon 66 (N66)	1815.61 ± 452.94	577.19 ± 259.06	355.42 ± 183.75	933.06 ± 192.51
Polyethylene (PE)	1789.33 ± 733.87	1055.82 ± 535.54	-	-
Polyethylene terephthalate (PET)	-	-	-	-
Acrylonitrile butadiene styrene (ABS)	-	3.96 ± 2.13	-	-
Polyurethane (PUR)	-	-	-	-
Styrene-butadiene rubber (SBR)	-	-	-	-
Polystyrene (PS)	-	-	-	-
ΣNMPs	**8925.72 ± 2590.50[a]**	**1636.97 ± 594.91[b]**	**355.42 ± 183.75[b]**	**966.71 ± 193.35[b]**

~2× higher than the other LMW PAHs (Table 1(a)). BaA was the most prominent HMW PAH in oysters, red drum and sea trout, with levels respectively 70×, 65×, and 26× higher than the remainder HMW PAHs (Table 1(a)). In catfish muscle, FLT and PYR were the most prominent HMW PAHs at 43× and 47× higher than the remaining HMW PAHs (Table 1(a)). While the sea trout muscle exhibited a near equivalent abundance for PYR and IcdP (19 % and 17 % respectively of the total HMW PAHs) (Table 1(a)).

In contrast to muscle, the liver tissue for all fish exhibited a predominance of LMW PAHs with the overall proportion of LMW PAHs constituting 69 %, 93 %, and 98 % to the ΣPAHs in catfish, red drum, and sea trout respectively (Table 2(a)). Of the LMW PAHs, FLU and ACE accounted for the most prominent congeners. While FLU accounted for 45 %, 70 %, and 81 % to the ΣPAHs in catfish, red drum, and sea trout respectively; ACE contributed 14 %, 21 %, and 15 % to the ΣPAHs in

Table 2
Fish liver concentrations of a) PAHs b) PCBs, and c) NMPs. Levels are reported in ng/g DW for PAHs and PCBs, and μg/g DW for NMPs (mean ± standard error). Levels below the limit of detection are represented by '-'. Different letters show significant differences ($p \leq 0.05$) between species. The analysis of NMPs in the livers of catfish was not possible due to a lack of sufficient tissue biomass remaining after the persistent pollutant (PAHs and PCBs) analysis.

	Catfish (n = 10)	Red drum (n = 7)	Sea trout (n = 3)
a) PAHs (ng/g DW)			
Low molecular weight (LMW)			
Acenaphthene (ACE)	94.99 ± 16.46	592.43 ± 194.09	431.40 ± 135.46
Fluorene (FLU)	307.02 ± 108.20	1969.08 ± 872.06	2287.88 ± 1498.61
Phenanthrene (PHE)	23.57 ± 9.34	47.20 ± 13.51	47.32 ± 23.96
Anthracene (ANT)	43.57 ± 4.04	24.24 ± 10.33	3.51 ± 1.82
High molecular weight (HMW)			
Fluoranthene (FLT)	52.87 ± 12.50	2.69 ± 1.35	0.84 ± 0.84
Pyrene (PYR)	41.69 ± 10.10	15.07 ± 4.27	19.61 ± 5.65
Benzo[*a*]anthracene (BaA)	29.71 ± 12.90	111.88 ± 79.47	3.98 ± 3.98
Chrysene (CHR)	34.44 ± 14.02	30.58 ± 16.55	2.43 ± 2.43
Benzo[*b*]fluoranthene (BbF)	1.60 ± 0.84	–	–
Benzo[*k*]fluoranthene (BkF)	2.22 ± 0.93	–	–
Benzo[*a*]pyrene (BaP)	6.80 ± 4.53	2.46 ± 1.45	4.09 ± 3.64
Indeno[1,2,3-*cd*] pyrene (IcdP)	21.94 ± 7.81	7.96 ± 1.81	11.62 ± 7.49
Dibenzo[*a,h*] anthracene (DahA)	15.62 ± 6.12	1.35 ± 0.95	–
Benzo[*g,h,i*]perylene (BghiP)	4.05 ± 1.28	12.85 ± 4.84	–
ΣPAHs	**680.08 ± 209.07[b]**	**2817.79 ± 1200.68[a]**	**2812.69 ± 1683.88[ab]**
b) PCBs (ng/g DW)			
Non-ortho (dioxin like)			
PCB 77	26.38 ± 12.34	42.66 ± 22.42	16.18 ± 11.80
PCB 81	7.61 ± 4.50	40.54 ± 26.05	3.00 ± 1.52
PCB 126	173.47 ± 63.13	3.09 ± 2.00	–
PCB 169	1.50 ± 1.01	–	–
Mono-ortho (dioxin like)			
PCB 105	22.95 ± 5.18	78.03 ± 26.82	17.50 ± 17.50
PCB 114	8.88 ± 4.53	191.38 ± 52.33	176.66 ± 84.50
PCB 118	7.95 ± 3.84	59.48 ± 29.65	19.52 ± 6.16
PCB 123	7.18 ± 3.15	45.13 ± 28.78	26.27 ± 21.98
PCB 156	0.47 ± 0.47	9.71 ± 3.89	1.56 ± 1.56
PCB 167	8.18 ± 5.66	50.70 ± 21.25	102.21 ± 22.51
PCB 189	0.40 ± 0.40	7.33 ± 5.45	–
Non-dioxin like			
PCB 1	40.01 ± 15.94	39.53 ± 11.21	44.64 ± 5.56
PCB 18	38.79 ± 11.65	1251.44 ± 654.69	65.06 ± 32.96
PCB 33	7.35 ± 2.81	26.66 ± 7.16	5.63 ± 0.73
PCB 52	–	–	–
PCB 95	17.04 ± 16.37	21.42 ± 13.44	–
PCB 101	4.07 ± 2.01	55.30 ± 19.29	17.00 ± 9.89
PCB 128	12.10 ± 10.19	87.85 ± 41.07	195.97 ± 39.44
PCB 138	–	0.87 ± 0.87	9.81 ± 3.97
PCB 149	–	7.69 ± 3.22	–
PCB 153	–	0.54 ± 0.54	0.33 ± 0.33
PCB 157	0.99 ± 0.66	5.46 ± 4.73	3.36 ± 1.71
PCB 170	–	2.62 ± 1.24	2.38 ± 2.38
PCB 171	–	1.87 ± 1.87	–

(*continued on next page*)

Table 2 (*continued*)

	Catfish (n = 10)	Red drum (n = 7)	Sea trout (n = 3)
PCB 177	–	0.68 ± 0.68	–
PCB 180	1.76 ± 1.28	1.42 ± 0.94	2.22 ± 2.22
PCB 183	2.33 ± 1.65	0.61 ± 0.61	–
PCB 187	3.35 ± 2.00	–	–
ΣPCBs	**392.76 ± 168.77[a]**	**2032.03 ± 980.20[a]**	**709.30 ± 266.72[a]**
c) NMPs (μg/g DW)			
Polymethyl methacrylate (PMMA)		–	–
Polypropylene (PP)		–	–
Polyvinyl chloride (PVC)		–	–
Polyamide (PA)		–	–
Polycarbonate (PC)		–	–
Nylon 66 (N66)		16,082.04 ± 6524.91	6536.69 ± 5176.33
Polyethylene (PE)		–	–
Polyethylene terephthalate (PET)		–	–
Acrylonitrile butadiene styrene (ABS)		–	–
Polyurethane (PUR)		–	–
Styrene-butadiene rubber (SBR)		2084.06 ± 1150.49	–
Polystyrene (PS)		–	–
ΣNMPs		**18,166.10 ± 6625.56[a]**	**6536.69 ± 5176.33[a]**

catfish, red drum, and sea trout respectively (Table 2(a)). For the HMW congeners, catfish exhibited high contributions of FLT (8 %), PYR (6 %), CHR (5 %), and BaA (4 %) to the ΣPAHs (Table 2(a)). In red drum and sea trout, only BaA (4 %) and PYR (1 %) contributed sufficiently to the ΣPAHs respectively (Table 2(a)).

PCBs body-burdens in the muscle and liver tissue of biota are detailed in Tables 1 and 2 respectively. The DL-PCBs comprised 44 %, 85 %, 28 %, and 33 % of ΣPCBs in oysters, catfish, red drum, and sea trout respectively (Table 1(b)). Overall, ΣPCBs in the gill/mantle tissue of oysters exhibited higher levels relative to those measured in muscle from catfish (11× higher, significant), red drum (2× higher, not significant), and sea trout (5× higher, not significant) (Table 1(b)). Amongst the fish species, red drum exhibited the highest ΣPCB levels (not significant) in muscle relative to catfish (6× higher) and sea trout (3× higher) (Table 1(b)). The livers of fish exhibited the highest ΣPCBs relative to the muscle, ranging from 11× to 15× higher in liver in comparison to muscle (Tables 1 and 2). The DL-PCBs comprised 67 %, 26 %, and 51 % of ΣPCBs in catfish, red drum, and sea trout respectively (Table 2(b)). The analysis of ΣPCBs in the livers of fish showed red drum to exhibit the highest levels (not significant) in comparison to catfish (5× higher) and sea trout (3× higher) (Table 2(b)).

3.3. Emerging pollutant body-burdens in biota

The ΣNMPs in the gill/mantle tissue of oysters had significantly higher body-burdens relative to muscle in fish, at levels 5× higher than catfish, 9× higher than sea trout, and 25× higher than red drum (Table 1 (c)). In oysters, PP was the most prominent NMP comprising 60 % of the ΣNMPs (Supplemental Fig. 3), with PE and N66 account for more than 25 % of the total NMP load. In catfish muscle tissues, PE dominated at 64 % of the ΣNMPs and in red drum and sea trout muscle, N66 predominated at ≥97 % of the ΣNMPs (Table 1(c)). The ΣNMP levels in the livers of red drum and sea trout were 51× and 7× higher than in their respective muscle tissues (Table 1(c) and Table 2(c)). Despite red drum exhibiting a mean level 3× that of sea trout, there were no significant differences between them (Table 2(c)). N66 was found to be prevalent in both red drum and sea trout liver (Supplemental Fig. 3). The analysis of NMPs in the livers of catfish was not possible due to a lack of sufficient tissue biomass remaining after the persistent pollutant (PAHs and PCBs) analysis.

4. Discussion

4.1. PAH body-burdens, sources, and toxicity risk assessment

Eastern oysters exhibited higher concentration of ΣPAHs per gram of tissue (230 ng/g DW compared to 124 to 198 ng/g DW in finfish (Table 1 (a)). The elevated PAH levels in shellfish in comparison to fish reported herein are consistent with observations from other aquatic ecosystems. For example, Rowe et al. (2020) measured ΣPAH levels in eastern oysters and finfish (spotted sea trout) from a neighboring bay system, Galveston Bay. Oysters had ΣPAHs levels of 203 ± 68 ng/g WW, mean ± standard error), while those reported in finfish were 14 ± 8 ng/g WW (Rowe et al., 2020). Even when accounting for differences between DW and WW, oysters accumulated more PAHs than finfish in these Texas estuaries. Such a trend is also evident in other aquatic ecosystems, for example, Kanhai et al. (2015), reported the ΣPAH levels in Mangrove oysters (*Crassostrea rhizophorae*) to be higher (109.0 ± 18.4 to 362.0 ± 63.0 ng/g DW) than those measured in sea catfish (*Cathorops spixii*) (7.5 ± 0.9 to 43.5 ± 25.5 ng/g DW) sampled from Caroni Swamp, Trinidad, West Indies. Interestingly, Olayinka et al. (2019) reported pink shrimp and blue marine crabs having an order of magnitude higher (50.6 ± 21.9 and 60.3 ± 15.7 μg/g) ΣPAH levels, along with fish (spadefish: 33.9 ± 9.2 μg/g, grunter: 35.0 ± 12.2 μg/g) in Atlast Cove, Nigeria. A recent comprehensive review by Honda and Suzuki (2020) comparing PAH body-burdens in shellfish and fish reported overall higher concentrations in invertebrates compared to vertebrates (fish), with ΣPAHs concentration in invertebrates ranging from 8.7 to 7000 ng/g WW and those in fish ranging from 1.52 to 1064 ng/g WW.

The higher body burden of pollutants in eastern oysters reported in our study likely reflects their filter feeding behavior, overall lipophilicity of PAHs, and lower metabolic biotransformation capacity of invertebrates (relative to finfish) to metabolize and excrete PAHs, as discussed below. Oysters have a massive capacity to filter ~25–50 gal of sea water per day (Ehrich and Harris, 2015; NOAA, 2020), which can increase their exposure to various contaminants including PAHs (Bustamante et al., 2012; Fisher et al., 2000; Trevisan et al., 2017; Wang et al., 2020). Invertebrates tend to have a lower biotransformation capacity for pollutants in comparison to fish, and therefore they are less efficient at metabolizing and depurating contaminants (Honda and Suzuki, 2020; Neff et al., 1976; Vidal-Liñán et al., 2016). The species-specific accumulation (from difference in diet, habitat, ability to expel pollutants) of various PAH congeners has reported by Neff et al. (1976), where the uptake and depuration of various oil derived PAHs (NAP, FLU, PHE etc.), across mollusk, shrimps and fish was studied. The authors reported that shrimp (*Penaeus aztecus*) and fish (*Fundulus similis*) were quick to accumulate as well as depurate PAHs, while oysters (*Crassostrea virginica*) and clams (*Rangia cuneata*) were slow to depurate, which resulted in higher body burdens in oysters and clams in comparison to shrimp and fish (Neff et al., 1976). Therefore, oysters may serve as an effective sentinel species for representing pollutant exposure in aquatic ecosystems.

In contrast to the muscle tissue in fish, their livers exhibited ΣPAH levels that were 5× to 14× higher (Table 2(a)). This is likely due to the lipophilic nature of PAHs (Sverdrup et al., 2002) and the higher lipid content in fish livers in comparison to muscle (Ando et al., 1993; Arrington et al., 2006). For example, in our study the gravimetrically determined lipid weight in livers was 4× higher than in muscle for catfish, 11× higher for sea trout, and 12× higher for red drum (data not shown). PAHs are hydrophobic (Log K_{ow} = 3.37–6.75) and highly lipophilic (Choi et al., 2010), therefore contributing to their accumulation in the liver tissue. The propensity of PAHs to preferentially accumulate in lipid rich tissues has also been shown in other studies. For example, in the Gulf of Mexico, where Blacktip and Bonnethead sharks were found to have 2× the bodyburden of PAHs in liver in comparison to muscle (Cullen et al., 2019). Our observed values were in range of the previously observed body burden of 500–1000 ng/g liver weight of

PAHs measured in the region (Sabine Lake) (Hernout et al., 2020). Elsewhere, Jafarabadi et al. (2019) showed ~1.4× higher PAH bioaccumulation in the livers, compared to muscle of fish collected from the Persian Gulf (such as red snapper, bream, and mackerel) (Jafarabadi et al., 2019). And a study from Poyang lake (China) also showed ~1.4× higher PAH levels in the liver compared to muscle of carp (Zhao et al., 2014). Xu et al. (2011) showed a significant positive correlation between tissue lipid content and PAH bioaccumulation, i.e., the brain exhibited greater PAH bioaccumulation in comparison to muscle.

In our study, LMW PAHs dominated in the liver, with ACE and FLU being the most prominent compounds, accounting for 25–75 % of all congeners (Supplemental Fig. 1(b)). ACE and FLU both have three aromatic rings, and have similar Log K_{ow} values (ACE = 3.92 and FLU = 4.18) (Jesus et al., 2022). The prevalence of LMW PAHs reflects the prominence of oil-derived hydrocarbons. For example, LMW PAHs primarily originate from petrogenic sources such as crude oil spills, petroleum products, and from the natural seepage of petroleum (Patel et al., 2020). While HMW PAHs are often products of pyrolytic sources, such as the combustion of petroleum, wood, coal etc. (Budzinski et al., 1997; Montuori et al., 2022; Wolska et al., 2012). Muscle exhibited a more mixed source of pollution with presence of LMW PAHs such as ACE, FLU and PHE (12–20 %) in as well as more HMW PAHs such as FLT (23 % in catfish), PYR (25 % in catfish), BaA (up to 38 % in oyster and reddrum) and IcdP (12–25 % in red drum and seatrout), often indicative of combustion from wood burning, vehicle and industrial activities. Similar mixed PAH profiles in biota have been observed in previous studies in northwestern GOM (Cullen et al., 2019; Hernout et al., 2020).

PAH ratios have been extensively used to diagnose their sources (Blumer, 1976; Budzinski et al., 1997; Lipiatou and Saliot, 1991; Simoneit, 1985; Yunker et al., 1999, 1996). The diagnostic source ratio analysis shown in Table 3 indicates an overall prominence of pyrogenic sources, with a 56 % average prominence of pyrogenic indicators across most species (with exception of oysters and seatrout liver). The ratios encompass complete and incomplete combustion of petroleum products with major contributions from maritime traffic, vehicle emissions, and industrial activity (TSHA, 2023). The bay serves as a hub for petrochemical shipping, with frequent oil tanker traffic and dredging operations that release PAHs through vessel engine combustion and petroleum-based residues (Tresaugue, 2014). The prominence of pyrogenic ratios, with also petrogenic indicators on oysters and seatrout livers reflect the dominance of combustion processes and also incidences of oil spills (i.e., petrogenic sources) along the Gulf of Mexico (HARC, 2014; Rice, 2019; Rowe et al., 2021; Trevizo, 2019). For example, the Calhoun Port Authority in Matagorda Bay received over 11.8 million tons of cargo in 2015, with its primary shipments consisting of petrochemicals, crude oil, condensate, and aluminum-related materials (bauxite and alumina) (TDT, 2020). The sources of PAHs in Matagorda Bay have been previously attributed to shipping activity in the area (Lloyd et al., 2024). In 2014, a cargo shipped collided with an oil tanker in Galveston Bay, near Texas city, which led to the spillage of fuel oil into lower Galveston Bay (DARRP, 2014; Williams et al., 2017), which then dispersed along shorelines of Galveston and Matagorda Bays (Tresaugue, 2014). Moreover, the Gulf of Mexico has experienced several significant oil spills that have had profound environmental and economic impacts. The most catastrophic was the Deepwater Horizon spill in 2010, where an explosion on the BP-operated drilling rig led to the release of approximately 4.9 million barrels (about 206 million gallons) of oil over 87 days, marking it as the largest marine oil spill in U. S. history (Beyer et al., 2016; Ramseur, 2010). The spike in LMW PAHs post oil spill and subsequent reduction back to base levels have been well documented in the region with the Deepwater horizon oil spill (Liu et al., 2012; Murawski et al., 2014; Romero et al., 2021; Snyder et al., 2015). Additionally, the Taylor Energy oil spill, which began in 2004 due to an underwater mudslide triggered by Hurricane Ivan, resulted in a continuous discharge of oil (estimated thousand gallons/week) from a production platform that persisted for over 16 years, becoming one of the longest-running oil spills in history in the Gulf of Mexico (Fears, 2018; Warren et al., 2014). In addition, heavy road traffic associated with the Port Lavaca–Point Comfort complex contributes PAHs via exhaust from trucks and plant vehicles. Industrial facilities in the area including Alcoa, Union Carbide, DuPont, and Formosa Plastics have historically emitted hydrocarbons, mercury, and chlorinated compounds through both accidental discharges and combustion processes (TSHA, 2023), which together reflect mixed sources of HMW and LMW PAHs exposure of biota in Matagorda Bay.

A cancer risk assessment was performed to determine whether consumption of Matagorda Bay seafood could cause sufficient exposure to carcinogenic PAHs, such as BaP and BaPE (ATSDR, 2022; Collins et al., 1991; EPA, 2017; FDA, 2010; Lee and Shim, 2007). The BaP and BaPE levels were below the minimum threshold for concern as established by the FDA after the Deepwater Horizon oil spill (FDA, 2010) (Fig. 2). Although widely adopted, a criticism of the FDA cancer risk level of concern approach is that it significantly underestimate risks to sensitive populations, including pregnant women, and children, by failing to account for increased vulnerability, appropriate consumption rates, relevant health endpoints, and health-protective exposure durations (Rotkin-Ellman et al., 2012; Solo-Gabriele et al., 2021).

4.2. PCB body-burdens and toxicity risk assessment

Similar to the trends observed for PAHs, our study also showed eastern oysters exhibit significantly higher levels of total PCBs compared to the muscle tissue of fish in Matagorda Bay. Specifically, PCB levels in oysters (290.29 ± 4.49 ng/g DW) were 11× higher than in catfish (26.25 ± 0.47 ng/g DW), 6× higher than redrum (158.53 ± 3.04 ng/g DW) and 2.5× higher than sea trout (64.04 ± 1.14 ng/g DW) (Table 1(b)). Similar to our findings, oysters collected from the Gulf of Mexico were reported to have up to 150 ng/g DW of PCBs following Hurricane Katrina and Rita (Johnson et al., 2009). Such a trend is also evident in other aquatic ecosystems. For example, in Todos os Santos Bay (Brazil), oysters exhibited ~10× higher PCB concentrations (<0.08–50 ng/g DW) compared to the fish sampled from the bay (0.23 to 4.55 ng/g DW)

Table 3
Diagnostic source analysis of PAHs in muscle and liver of biota (oyster and fish) using various ratios of LMW to HMW PAHs. The table also mentions the levels at which the source is considered to be pyrogenic (Tobiszewski and Namieśnik, 2012). The presence of * beside a value means the ratio indicates it is predominantly pyrogenic.

Diagnostic ratios	Pyrogenic* if	Oyster	Catfish muscle	Reddrum muscle	Seatrout muscle	Catfish liver	Reddrum liver	Seatrout liver
∑LMW/∑HMW	<1	0.51*	0.88*	0.41*	0.88*	1.70	22.59	58.05
∑COMB/∑PAH	~1	0.66	0.53	0.71	0.53	0.37	0.04	0.02
FLT/(FLT + PYR)	>0.4	0.00	0.47*	0.00	0.00	0.54*	0.00	0.00
ANT/(ANT+PHE)	>0.1	0.04	0.38*	0.34*	0.23*	0.80*	0.19*	0.06
BaA/(BaA + CHR)	>0.2	0.74*	–	1.00*	–	0.34*	0.65*	–
IcdP/(IcdP+BghiP)	>0.2	0.17	–	1.00*	1.00*	0.72*	0.31*	1.00*
PHE/ANT	<10	22.17	1.61*	1.98*	3.38*	0.25*	4.32*	14.52
Pyrogenic*[a]		29 %	**80 %**	**71 %**	**67 %**	**71 %**	**57 %**	17 %
Petrogenic		**71 %**	20 %	29 %	33 %	29 %	43 %	**83 %**

[a] Bold text represents the dominant source of PAH (Petrogenic/ Pyrogenic)

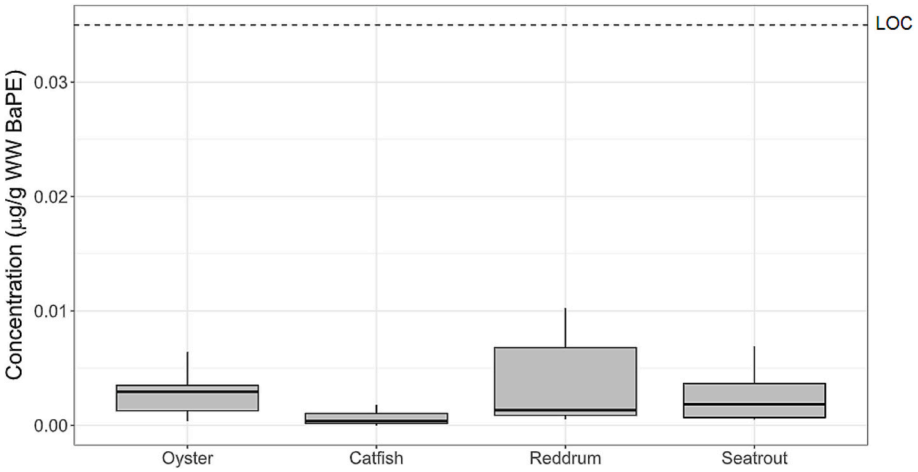

Fig. 2. Box and whisker plots of cancer risk level of concern (LOC) set by the FDA for finfish (0.035 µg/g BaPE) is shown as a horizontal dotted line and is compared to the Benzo [a]pyrene equivalent toxicity (BaPE) concentrations of finfish and oysters collected from Matagorda Bay. The FDA LOC level for oysters (0.142 µg/g BaPE) is not shown.

(Santos et al., 2020). Similarly, fish (*Plastycephalus bassensis*) and oysters (*Crassostrea gigas*) sampled from Tasmanian estuarine and coastal waters revealed oysters to exhibit 5× higher total PCBs levels than the fish. Similar to PAHs, the higher body-burdens of PCBs in oysters is likely a reflection of their filter feeding capacity (Ehrich and Harris, 2015; NOAA, 2020), overall higher lipophilicity of PCBs (Bourez et al., 2013; Safe and Hutzinger, 1984), and lower metabolic biotransformation capacity of invertebrates (relative to finfish) to metabolize and excrete PCBs (Bright et al., 1995; Vidal-Liñán et al., 2016).

In contrast to muscle tissue, the livers of fish exhibited 11-15× higher PCB levels (Table 2(b)). The higher levels in livers reflect the lipophilic nature of PCBs (Bourez et al., 2013; Safe and Hutzinger, 1984) and the higher lipid content of the livers in comparison to muscle (as previously discussed for PAHs) (Ando et al., 1993; Arrington et al., 2006). PCBs are highly lipophilic (Log K_{ow} = 4.43–5.02) (Ballschmiter et al., 2005). Similar to the case of PAHs, in the Gulf of Mexico, Bull, Blacktip and Bonnethead sharks were found to have 2× the bodyburden of PCBs in liver in comparison to muscle (Cullen et al., 2019). Our observed values were in range of the previously observed Sabine lake gaftopsail catfish and red drum body burden of 500–1000 ng/g LW of PCBs (Hernout et al., 2020). Similarly in other industrial regions, Bodin et al. (2014) have shown hepatic PCB levels to be 10× higher than the muscle tissue of fish sampled from the Gironde estuary in southwest France (Bodin et al., 2014). Monosson et al. (2003) collected muscle, liver and gonad tissue from mummichog fish (*Fundulus heteroclitus*) from Hudson river and Newark bay and found total PCB levels in the gonads and livers (1265–3453 ng/g WW total PCBs) to be ~6-13× higher than levels measured in muscle tissue (209–263 ng/g WW). They attributed the tissue specific differences to be due to the high lipophilicity of PCBs and higher lipid content of livers (Monosson et al., 2003). Similarly, the analysis of fish muscle, liver, kidney and brain from a heavily polluted water reservoir in Slovakia (Zemplinska sirava) found total PCB concentrations in the liver to be 2× higher than in muscle, and 15× higher than in the brain and kidneys (Brázová et al., 2012). Moreover, PCBs measured in the muscle, and liver of Red mullet, mackerel, anchovy and blue whiting along the Catalan coast of the Mediterranean Sea, reported livers to exhibit 10× higher concentrations of total PCBs than muscle (Albaiges et al., 1987).

PCBs are exclusively of anthropogenic origin and were widely used in heat absorbing or electrical/insulating materials such as electrical equipment, capacitors, and transformers (Delzell et al., 1994). Despite their ban in the 1970's, they continue to persist in the environment due to their resistance to biodegradation (Boyle and Highland, 1979). The high chlorination of PCBs results in chemical and structural properties that collectively reduce the susceptibility of PCBs to chemical, biological, and photolytic degradation pathways, thus increasing their environmental persistence, which explains their prevalence and designation as a persistent pollutant (Delzell et al., 1994; Elangovan et al., 2019; Xiang et al., 2020). DL- PCBs are those with chlorine atoms at the *para* position (opposite sides of the benzene ring) and two or more at the *meta* positions (adjacent but not next to on the benzene ring) (ATSDR, 2023; Safe et al., 1985). Chlorine atom substitutions in these position results in a coplanar structure similar to that of 2,3,7,8-TCDD (2,3,7,8-tetrachlorodibenzodioxin), and thus exhibit its high toxicity (Safe et al., 1985). These include non-ortho dioxin like PCBs such as, 3,4,4′,5-tetra- (PCB 81), 3,3′,4,4′-tetra- (PCB 77), 3,3′,4,4′,5-penta- (PCB 126), and 3,3′,4,4′,5,5′-hexachlorobiphenyl (PCB 169) and mono-ortho dioxin-like PCBs such as PCBs 105, 114, 118, 123, 156, 167 and 189 (Giesy and Kannan, 1998). In oysters, PCB 77 dominated constituting 49 % of total DL-PCBs (Table 1(b)). For the fish, catfish showed a similar prominence of PCB 126 in both muscle and liver tissue, at ~60 % of total DL-PCBs (Tables 1 and 2(b)). The livers of red drum and sea trout showed a prominence PCB 114 in each species (36 % and 49 % respectively) (Table 2(b)). Whereas PCB 156 dominated in red drum muscle (26 % of total DL-PCBs) and PCB 105 dominated in sea trout muscle (35 % of total DL-PCBs) (Also see Supplemental Fig. 2). The prominence of DL-PCBs is typical of industrialized aquatic ecosystems. For example, Carro et al. (2018) report in DL-PCBs in bivalve mollusks collected from estuaries along Galician Rias in Northwestern Spain to comprise 72 % of the total PCBs. Amongst the DL-PCB congeners, 93 % were contributed by PCB 126 (Carro et al., 2018). In another study, DL-PCBs were also detected at higher concentrations than NDL-PCBs in commercially available finfish and shellfish, accounting for up to 96 % of the PCBs in tuna and 90 % in oysters (Gómara et al., 2005). Gómara et al. (2005), also reported PCB 126 to be the most prominent congener in finfish and shellfish. A study from coastal Korea (Busan, Incheon, Pohang, Ulsan) focusing on the PCB content of fish and bivalves found that up to 60 % of the dietary intake of PCBs to the Korean population from seafood was from DL-PCBs, and of which PCB-126 was also the most prominent congener (Moon and Ok, 2006).

Amongst the NDL-PCBs in the muscle tissue of fish (or gill/mantle for oysters), we find PCB 18 to be the most commonly (and prominently) detected PCB congener, ranging from 60 % to 76 % of the total NDL-PCBs (Table 1(b), Supplemental Fig. 2). For the NDL-PCBs in the livers of fish, we also find PCB 1 to dominate in catfish (31 % of the total NDL-PCBs), PCB 18 was the most abundant in red drum livers (83 % of total), and PCB 128 dominated in sea trout livers (57 % of total). The varying ratios of NDL-PCBs may reflect varying extents of microbial anaerobic

degradation of highly chlorinated PCBs, resulting in the removal of chlorines from the *meta* and *para* positions. This results in an increase in lower chlorinated *ortho*-substituted PCB congeners such as PCBs 18, 52, and 128 (Abramowicz, 1995; Tiedje et al., 1993). Therefore, the prevalence of PCB 18 and PCB 128 in the biota may reflect biodegradation of dioxin like PCBs via anaerobic bacteria. The analysis of PCB congeners in the muscle and liver tissues of sharks sampled from Galveston Bay (TX, USA) have reported PCB 128 body-burdens to range from 4 to 28 % (Cullen et al., 2019). Hernout et al. (2020) has shown a prevalence of PCB 18 in the livers of fish (~20–65 %) sampled from Sabine Lake (TX, USA) (Hernout et al., 2020). Finally, Finklea et al. (2000) analyzed PCBs in the blubber of stranded bottlenose dolphins from Matagorda Bay (TX, USA). Their analysis revealed the prevalence of PCB 128 (≤1400 ng/g of LW). All these studies demonstrate the prevalence of select PCB congeners in biota sampled along Matagorda Bay. Ongoing industrial discharges and the remobilization of historically contaminated sediments may continue to contribute to dioxin pollution despite regulations. Additionally, sediment resuspension from tides, wind, shipping, and dredging reintroduces previously buried persistent dioxins into the environment as observed in the case of Galveston Bay shipping channel (Yeager et al., 2007).

The TEQ analysis showed red drum to be within the range of the upper and lower limits for adverse effects in finfish, suggesting the propensity of the DL-PCBs body-burdens to cause adverse effects on this species (Fig. 3). For the sea trout, the TEQ was 1.4× lower than the low limit for adverse effects in finfish, indicating a significantly lower risk of adverse effects (i.e., protective of ≥99 % of fish). A previous study out of Sabine Lake (Texas and Louisiana coast) reported TEQ values of red drum and gaftopsail catfish to be within the range of upper and lower thresholds for finfish toxicity (Hernout et al., 2020). For catfish, the TEQ levels were 1.11× higher than the upper limit for adverse effects set for finfish, indicating a potential health risk (such as immunosuppression effects) to the catfish (i.e., ≥10 % may show adverse effects) (Kannan et al., 2000). At these levels, adverse effects such as suppression of lymphocytes, natural killer cell, plasma concentration of vitamin A, and thyroid hormones have been reported (Kannan et al., 2000). The high TEQ values in catfish are likely representative of the high PCB 126 body-burdens in livers (65 % of total DL-PCBs) (Table 2(b)). Not all the congeners in the TEQ calculation have equal TEF values due to their relative toxicity and therefore are "weighed" differently. Of the DL-PCBs, PCB 126 exhibits the highest TEF value at 10–1000× higher than the others, therefore contributing to the high TEQ values observed in catfish. A caveat is that TEF standards for DL-PCBs are derived from studies on early life stage fish with mortality as an endpoint (Vandermeulen, 1987). Therefore, the derived TEQ values may not be directly applicable towards explaining sub-lethal toxicity effects in older finfish (as is this case in our study). Furthermore, the present TEQ assessment method cannot explain the toxic effects derived from non-dioxin like PCBs which may still have carcinogenic, neurotoxic, and endocrine disruptive effects at higher concentrations (Giesy and Kannan, 1998; Safe, 1994). Therefore, TEQ assessment values need to be interpreted with caution.

4.3. NMP body-burdens and average human daily intake

This is one of the first comprehensive reports of NMPs (using Py-GCMS/MS) in eastern oysters and fish collected from Matagorda Bay. Oysters exhibited significantly higher body-burdens of NMPs (8925.72 ± 2608.77 μg/g DW) compared to fish muscle (355.42–1636.97 μg/g DW) as previously seen in the case of both PAHs and PCBs (Table 1(c)). The higher body burden of NMPs in oysters is likely a direct reflection of their filter feeding capacity (Ehrich and Harris, 2015; NOAA, 2020) as discussed previously. In Sanggou Bay, China, Pacific oysters also exhibited higher concentrations of NMPs than those detected in greenling (Sui et al., 2024). In fish livers (6536.69–18,166 μg/g DW), the concentration of NMPs was significantly higher than those in the muscle tissue. These differences in NMPs body-burdens may be due to the liver's rich blood supply and its primary role in filtering (and detoxifying) exogenous substances from the blood (Ozougwu, 2017; Wisse et al., 1985; Wood, 2014; Zhao et al., 2014), leading to a higher exposure and bioaccumulation in the liver. A toxicological study exposing European seabass (*Dicentrarchus labrax*) to NMPs (≤3 μm particle size) for ≤5 days showed approximately 4× and 3× higher microplastics accumulation in the liver compared to the gut and gills respectively (Zitouni et al., 2021). Similarly, goldfish exposed to NMPs (for 30 days) and exhibited a ~14× higher bioaccumulation in the liver compared to muscle tissue (Brandts et al., 2022). Additionally, various fish species sampled from the Pearl river in China (such as carp, bream, catfish, tilapia) were found to contain ~2× higher levels of plastics additives in their livers in comparison to muscle (Peng et al., 2021).

Amongst the plastics, Nylon-66 (N66) was the most prominently detected plastic in oysters (gill/mantle) and fish (muscle and liver). N66 is primarily used in textiles and fabrics, including carpets, clothing, and upholstery, due to its durability and resistance to wear and tear. It is also used in engineering plastics for automotive and industrial components like gears, bushings, and bearings, as well as in consumer goods like ropes, cords, fishing gear, nets and toothbrush bristles (Shakiba et al., 2021; Stafford et al., 1986; Zhang et al., 2010). We also show Polyethylene to account for 25 % of NMPs in both catfish muscle and oyster

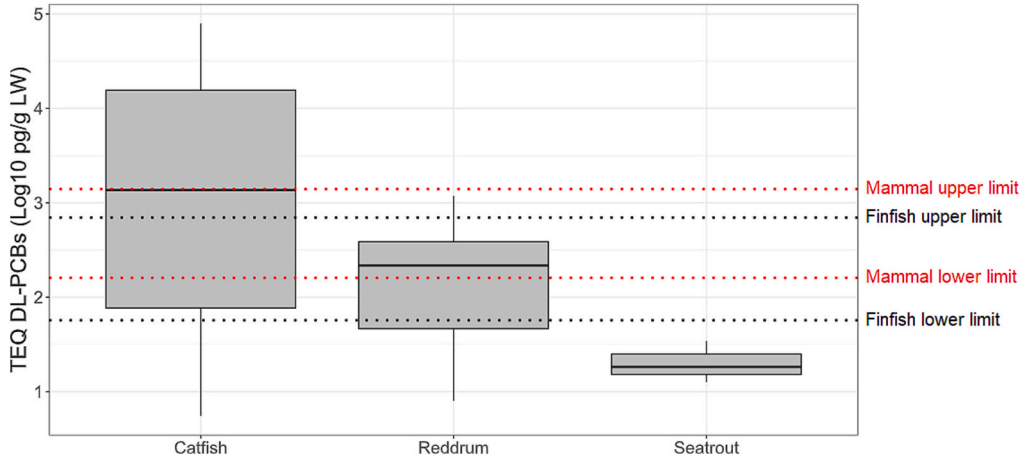

Fig. 3. Box and whisker plots of TEQ assessment for DL-PCBs in fish livers displayed with the upper and lower limit of adverse effects for finfish (black dotted lines) and aquatic mammals (red dotted lines) reported in Log10 transformed pg/g lipid weight (or pg/g LW TEQ). (For interpretation of the references to color in this figure legend, the reader is referred to the web version of this article.)

gill/mantle tissues. The prominence of Polyethylene highlights the presence of general plastics degradation products, including those from plastic pellets such as nurdles (OSPAR, 2018). Polyethylene is widely used in packaging materials such as plastic bags, films, bottles, containers, pipes, fittings, and medical applications due to their flexibility (Duffy Jr, 1949; Ronca, 2017; Savas et al., 2016). Polypropylene constituted 40 % of the NMPs detected in oysters from Matagorda Bay. Polypropylene is commonly used in packaging materials like bottles and containers, automotive parts such as bumpers and battery cases, textiles for items like diapers and filters, and household goods including reusable containers and furniture (Guidetti et al., 1996; Hossain et al., 2024; Maddah, 2016). The prevalence of Polypropylene and Polyethylene in aquatic biota has been previously reported by Ribeiro et al. (2020) in Australia. Polyethylene was the most prevalently detected plastic in the biota (≤2400 μg/g WW tissue), and Polypropylene was less common: ≤60 μg/g tissue (Ribeiro et al., 2020). A meta-analysis on the extent of microplastics ingested by fish worldwide conducted by Lim et al. (2022), found that majority ingested were fibrous microplastics (70 %), of which 16 % were Polyethylene (Lim et al., 2022).

Of importance, Polypropylene and Polyethylene, which were commonly detected in the biota from Matagorda Bay, were also some of the most widely produced plastics by the Formosa Plastics Corporation chemical plant located in Point Comfort (near sampling site A, Fig. 1), along Matagorda Bay (Detore, 2018; Hays, 2019). The Formosa Plastics Corporation (headquartered in Taiwan) is a major producer of plastic resins and petrochemicals, including PP, PE, and PVC. Their Point Comfort facility is significant for their operations in the United States (Conkle, 2018). In 2016, a substantial spill of plastic pellets and powder from this facility contaminated Matagorda Bay, leading to a lawsuit by environmental activist Ms. Diane Wilson (Wilson, 2018). In 2019, Formosa was found liable for illegal discharges, resulting in a $50 million settlement for environmental cleanup (Conkle, 2018; Wilson, 2018). Additionally, Formosa Plastics has been involved in other serious incidents. In 2005, an explosion at their Illinois plant producing PVC caused five fatalities (OSHA, 2005). In 2013, a fire at the Point Comfort facility resulted in injuries and environmental harm (CSB, 2006). The company has also faced scrutiny for air pollution violations, leading to fines and mandated corrective actions (EPA, 2012).

The ADIs calculated in this study for likely human exposures to microplastics through seafood consumption maps the NMPs body-burdens to an estimated daily intake of seafood (DSHS, 2011). As a result, the estimated ADIs for the NMPs varies from 0.03 to 0.46 mg NMPs/kg body weight/day for the consumption of red drum to oysters. The levels computed herein are relatively modest as compared to another study that estimated plastics ingestion rates by humans of ≤5 g of microplastics/week (or ≤ 260 g of microplastics/year) (Senathirajah et al., 2021). We are however within range of a study by Ribeiro et al. (2021), who deployed oysters (*Saccostrea glomerata*) at the mouth of Brisbane River (Australia) for 14 days and quantified a body-burden of ≤38.8 mg/g microplastics in the oysters and using an analytical method similar to the one in our study, i.e., Py-GCMS. The microplastics accumulated in oysters over 14 days can be approximated to a daily body burden of ≤2.8 mg/g oyster (by dividing 38.8 mg/g by 14). Implementing a similar ADI approach to the one taken in our study yields an average daily intake of 1.2 mg NMPs/kg body weight/day, and annual intake of 434 mg NMPs/kg body weight/year. These values are only 3× higher than the ones computed for the oysters sampled from Matagorda Bay in this study (Table 4).

A caveat to these estimates is that they appear to far exceed levels detected in the body-burdens of humans. For example, Leslie et al. (2022) used Py-GCMS to quantify NMPs in human blood and reported total levels of 1.6 μg/mL. While NMPs measurements in blood are not comparable to tissue body-burdens in wildlife biota as measured in our study, nevertheless the levels measured by Leslie et al. (2022) are ~200× lower than the lowest NMP body burden measured for red drum muscle in our study (i.e., 355.42 ± 183.75 μg/g DW). In another study, the quantification of microplastics in infant and adult human feces reported concentrations ranging from 3 to 36 μg/g (Zhang et al., 2021). Once again, comparing these levels to the lowest NMP body-burden quantified for red drum muscle yields levels in humans that are ~10×–100× lower than those measured in fish. The differences in NMPs body-burdens between the aquatic wildlife (as measured in our study) and humans may indicate a trophic dilution of NMPs in an ecosystem. For example, we report that oysters exhibit ~5× – 25× higher body-burdens than fish (i.e., catfish, red drum, and sea trout), whereas fish (red drum) exhibits a ~ 10× – 200× higher body-burden than humans. Further studies applying the Py-GCMS analytical method to quantify NMPs across food webs which include wildlife biota and humans, will provide a more comprehensive assessment of the fate and distribution of these emerging pollutants in ecosystems.

Table 4
The estimated average daily intake (ADI) of NMPs in an adult human represented as mg NMPs/kg of body weight/day. The ADI data is shown per species with the minimum (min) and maximum (max) daily intakes also shown. Each ADI value was also converted to a yearly intake to assess the likely annual exposure of a person to NMPs.

Species	ADI (min–max) (mg NMPs/kg body weight/day)	Yearly intake (min–max) (mg NMPs/kg body weight/year)
Oysters	0.46 (0–1.47)	167.00 (1.72–536)
Catfish	0.15 (0–0.69)	55.6 (0–253)
Red drum	0.03 (0–0.13)	12.08 (0–46.9)
Sea trout	0.09 (0.02–0.18)	32.8 (7.80–65.7)

5. Conclusions

In this study, we report on the body-burdens of persistent (PAHs, PCBs) and emerging (NMPs) pollutants in shellfish and fish from Matagorda Bay (Texas, USA). The pollutant levels were quantified in muscle (gill/mantle of oysters) and liver tissues. Overall, the oysters exhibited higher levels of PAHs and PCBs relative to that of fish. The higher exposure of oysters to the persistent pollutants is likely due to their massive filter-feeding capacity (~25–50 gal of seawater/day), lipophilicity of the persistent pollutants, and/or low biotransformation capacity of the shellfish compared to fish. For PCBs, the liver tissue of fish exhibited ten-times higher levels than muscle. The assessment of PAH congeners indicated the prevalence of both LMW and HMW PAHs from petrogenic and pyrogenic sources. For the PCB congeners, there was an overall prominence of DL-PCBs, with PCB-126 contributing up to ~60 % of DL-PCBs in catfish muscle and liver. As a result, the TEQ levels for catfish were higher than the upper limit for adverse effects set for finfish, indicating a potential health risk to humans consuming these fish. A key result of this study was the quantification of NMP body-burdens that were ~ 2000× - 60,000× higher than those for PAHs and PCBs. Once again, oysters exhibited higher NMPs body-burdens (5-25×) than the levels measured in fish muscle. The most commonly detected NMPs in the body-burdens of biota were Nylon 66, Polypropylene and Polyethylene. Their prevalence is likely reflective of the legacy plastics pollution of Matagorda Bay by the Formosa Plastics Corporation, which was responsible for a substantial spill of plastic pellets and powder in 2016. Even though the NMPs were measured at orders of magnitude higher concentrations than the persistent pollutants (PAHs and PCBs), the toxicity implications of such high exposure of the resident biota are presently unknown due to a lack of standardized risk assessment methods or tests for plastics, which constitutes an avenue for further monitoring and research.

CRediT authorship contribution statement

Asif Mortuza: Writing – review & editing, Writing – original draft,

Visualization, Software, Methodology, Investigation, Formal analysis, Data curation, Conceptualization. **Emily N. Meese:** Writing – review & editing, Resources, Investigation, Data curation. **Marcus Wharton:** Resources, Methodology. **Bryan Gahn:** Software, Methodology, Investigation, Formal analysis, Data curation. **Lene H. Petersen:** Supervision, Resources, Project administration, Funding acquisition, Conceptualization. **Antonietta Quigg:** Writing – review & editing, Resources, Project administration, Funding acquisition, Conceptualization. **R.J. David Wells:** Resources, Project administration, Funding acquisition, Conceptualization. **Karl Kaiser:** Validation, Supervision, Software, Resources, Project administration, Methodology, Investigation, Funding acquisition, Formal analysis, Conceptualization. **David Hala:** Writing – review & editing, Writing – original draft, Validation, Supervision, Software, Resources, Project administration, Methodology, Investigation, Funding acquisition, Formal analysis, Conceptualization.

Declaration of competing interest

The authors declare that they have no known competing financial interests or personal relationships that could have appeared to influence the work reported in this paper.

Acknowledgements

The research presented in this manuscript was supported by the Matagorda Bay Mitigation Trust (Grant# 0013) to Hala, Kaiser, Wells, Quigg, Petersen; in part by the Texas Comptroller of Public Accounts funding (Grant# CMD 19-6799CS) to Wells; and in part by the U.S. Army Corps of Engineers Grant# ERDC BAA 21-0045A to Kaiser.

Appendix A. Supplementary data

Supplementary data to this article can be found online at https://doi.org/10.1016/j.marpolbul.2025.118495.

Data availability

The data supporting the findings of this study have not been made publicly available. However, upon request can be shared by the corresponding author.

References

Abramowicz, D.A., 1995. Aerobic and anaerobic PCB biodegradation in the environment. Environ. Health Perspect. 103 (Suppl. 5), 97–99.
Albaiges, J., Farran, A., Soler, M., Gallifa, A., Martin, P., 1987. Accumulation and distribution of biogenic and pollutant hydrocarbons, PCBs and DDT in tissues of western Mediterranean fishes. Mar. Environ. Res. 22 (1), 1–18.
Anchondo, C., 2019. Environmentalists take petrochemical giant Formosa to court over plastics pollution, The Texas Tribune. https://www.texastribune.org/2019/03/25/formosa-goes-to-federal-court-for-alleged-plastic-pollution/.
Ando, S., Mori, Y., Nakamura, K., Sugawara, A., 1993. Characteristics of lipid accumulation types in five species of fish. Nippon Suisan Gakkaishi 59, 1559–1564.
Arman, N.Z., Salmiati, S., Aris, A., Salim, M.R., Nazifa, T.H., Muhamad, M.S., Marpongahtun, M., 2021. A review on emerging pollutants in the water environment: existences, health effects and treatment processes. Water 13 (22), 3258.
Arrington, D.A., Davidson, B.K., Winemiller, K.O., Layman, C.A., 2006. Influence of life history and seasonal hydrology on lipid storage in three neotropical fish species. J. Fish Biol. 68, 1347–1361.
ATSDR, 2022. Guidance for calculating benzo(a)pyrene equivalents for cancer evaluations of polycyclic aromatic hydrocarbons, DHHS. https://www.atsdr.cdc.gov/pha-guidance/resources/ATSDR-PAH-Guidance-508.pdf.
ATSDR, 2023. What are polychlorinated biphenyls (PCBs)?, Center for Disease Control. https://www.atsdr.cdc.gov/csem/polychlorinated-biphenyls/what_are.html.
Ballschmiter, K., Klingler, D., Ellinger, S., Hackenberg, R., 2005. High-resolution gas chromatography retention data as a basis for estimation of the octanol–water distribution coefficients (K ow) of PCB: the effect of experimental conditions. Anal. Bioanal. Chem. 382, 1859–1870.
Barron, M.G., Heintz, R., Rice, S.D., 2004. Relative potency of PAHs and heterocycles as aryl hydrocarbon receptor agonists in fish. Mar. Environ. Res. 58 (2), 95–100. https://doi.org/10.1016/j.marenvres.2004.03.001 (2004/08/01).
Berdutina, A., Neklyudov, A., Ivankin, A., Karpo, B., Mitaleva, S., 2000. Comparison of proteolytic activities of the enzyme complex from mammalian pancreas and pancreatin. Appl. Biochem. Microbiol. 36, 363–367.
Beyer, J., Trannum, H.C., Bakke, T., Hodson, P.V., Collier, T.K., 2016. Environmental effects of the Deepwater Horizon oil spill: a review. Mar. Pollut. Bull. 110 (1), 28–51.
Bhattacharya, A., Khare, S., 2022. Ecological and toxicological manifestations of microplastics: current scenario, research gaps, and possible alleviation measures. J. Environ. Sci. Health C 38 (1), 1–20.
Blumer, M., 1976. Polycyclic aromatic compounds in nature. Sci. Am. 234 (3), 34–45.
Bodin, N., Tapie, N., Le Ménach, K., Chassot, E., Elie, P., Rochard, E., Budzinski, H., 2014. PCB contamination in fish community from the Gironde Estuary (France): blast from the past. Chemosphere 98, 66–72.
Bourez, S., Van den Daelen, C., Le Lay, S., Poupaert, J., Larondelle, Y., Thomé, J.-P., Schneider, Y.-J., Dugail, I., Debier, C., 2013. The dynamics of accumulation of PCBs in cultured adipocytes vary with the cell lipid content and the lipophilicity of the congener. Toxicol. Lett. 216 (1), 40–46.
Boyle, R.H., Highland, J.H., 1979. The persistence of PCBs. Environ. Sci. Policy Sustain. Dev. 21 (5), 6–37.
Brandts, I., Cánovas, M., Tvarijonaviciute, A., Llorca, M., Vega, A., Farré, M., Pastor, J., Roher, N., Teles, M., 2022. Nanoplastics are bioaccumulated in fish liver and muscle and cause DNA damage after a chronic exposure. Environ. Res. 212, 113433.
Brázová, T., Hanzelová, V., Miklisová, D., Šalgovičová, D., Turčeková, Ľ., 2012. Biomonitoring of polychlorinated biphenyls (PCBs) in heavily polluted aquatic environment in different fish species. Environ. Monit. Assess. 184, 6553–6561.
Bright, D.A., Grundy, S.L., Reimer, K.J., 1995. Differential bioaccumulation of non-ortho-substituted and other PCB congeners in coastal Arctic invertebrates and fish. Environ. Sci. Technol. 29 (10), 2504–2512.
Budzinski, H., Jones, I., Bellocq, J., Pierard, C., Garrigues, P., 1997. Evaluation of sediment contamination by polycyclic aromatic hydrocarbons in the Gironde estuary. Mar. Chem. 58 (1–2), 85–97.
Burns, E.E., Boxall, A.B.A., 2018. Microplastics in the aquatic environment: evidence for or against adverse impacts and major knowledge gaps. Environ. Toxicol. Chem. 37 (11), 2776–2796. https://doi.org/10.1002/etc.4268.
Bustamante, J., Arana, G., de Diego, A., Madariaga, J.M., 2012. The use of SPMDs and implanted oysters for monitoring PAHs and PCBs in an aquatic environment in the estuary of Urdaibai (Western Pyrenees). Environ. Eng. Manag. J. 11 (9), 1707–1714.
Cantillo, A.Y., 1997. World Mussel Watch Data.
Carro, N., García, I., Ignacio, M., Mouteira, A., 2018. Polychlorinated dibenzo-P-dioxins and dibenzofurans (PCDD/Fs) and dioxin-like polychlorinated biphenyls (dl-PCBS) in bivalve mollusk from Galician Rías (NW, Spain). Chemosphere 197, 782–792.
census.gov, 2019. Coastline America. https://www.census.gov/content/dam/Census/library/visualizations/2019/demo/coastline-america.pdf. (Accessed 5 January 2023).
Choi, H., Harrison, R., Komulainen, H., Saborit, J.M.D., 2010. Polycyclic aromatic hydrocarbons. In: WHO Guidelines for Indoor Air Quality: Selected Pollutants. World Health Organization.
Collins, J., Brown, J., Dawson, S., Marty, M., 1991. Risk assessment for benzo [a] pyrene. Regul. Toxicol. Pharmacol. 13 (2), 170–184.
comptroller.texas.gov, 2020. Manufacturing in the Gulf Coast region. https://comptroller.texas.gov/economy/economic-data/manufacturing/2020/gulf-coast.php. (Accessed 5 January 2024).
Conkle, J.L., 2018. San Antonio Bay estuarine waterkeeper and S. Diane Wilson vs. Formosa Plastics Corp, TCEQ. https://www.tceq.texas.gov/downloads/permitting/water-quality-standards-implementation/conkle-dr-ex-33.pdf.
CSB, 2006. Chemical Safety Board (CSB): CSB issues case study of Formosa Plastics Point Comfort, Texas, fire and explosions: unprotected piping, non-fireproofed structures, lack of automatic shutoff valves noted as causes; flame-resistant clothing recommended. https://www.csb.gov/csb-issues-case-study-of-formosa-plastics-point-comfort-texas-fire-and-explosions-unprotected-piping-non-fireproofed-structures-lack-of-automatic-shutoff-valves-noted-as-causes-flame-resistant-clothing-recommended/. (Accessed 20 January 2025).
Cullen, Marshall, C.D., Hala, D., 2019. Integration of multi-tissue PAH and PCB burdens with biomarker activity in three coastal shark species from the northwestern Gulf of Mexico. Sci. Total Environ. 650 (Pt 1), 1158–1172. https://doi.org/10.1016/j.scitotenv.2018.09.128 (Feb 10).
Dailey, J., 1977. Trends in spotted seatrout and red drum abundance in Texas coastal waters influenced by commercial netting activities. In: Proc. Annual Conf. SE Assoc. Fish & Wildlife Agencies.
DARRP, 2014. Texas City Y|Oil Spills|Damage Assessment, Remediation, and Restoration Program, NOAA. https://darrp.noaa.gov/oil-spills/texas-city-y.
Deblonde, T., Cossu-Leguille, C., Hartemann, P., 2011. Emerging pollutants in wastewater: a review of the literature. Int. J. Hyg. Environ. Health 214 (6), 442–448. https://doi.org/10.1016/j.ijheh.2011.08.002 (2011/11/01).
Delzell, E., Doull, J., Giesy, J., Mackay, D., Munro, I., Williams, G., 1994. Polychlorinated biphenyls. Regul. Toxicol. Pharmacol. 20, S187–S307.
Detore, D., 2018. Formosa: PE, PP capacity expansions underway in Texas, Plastics News. https://www.plasticsnews.com/article/20180507/NEWS/180509915/formosa-pe-pp-capacity-expansions-underway-in-texas.
DSHS, 2011. Characterization of potential adverse health effects associated with consuming fish from Sabine Lake, Texas. https://www.dshs.texas.gov/sites/default/files/seafood/PDF2/Risk-Characterization/Sabine-Lake-RC-2010.pdf.
Duffy Jr., B., 1949. The clinical use of polyethylene tubing for intravenous therapy: a report on seventy-two cases. Ann. Surg. 130 (5), 929.
Ehrich, M.K., Harris, L.A., 2015. A review of existing eastern oyster filtration rate models. Ecol. Model. 297, 201–212.

Elangovan, S., Pandian, S.B.S., SJ, G., Joshi, S.J., 2019. Polychlorinated biphenyls (PCBs): environmental fate, challenges and bioremediation. In: Microbial Metabolism of Xenobiotic Compounds, pp. 165–188.
EPA, 2012. Case summary: settlement with Formosa Plastics Corporation for site-wide corrective actions at Point Comfort, Texas Facility, United States Environmental Protection Agency. https://www.epa.gov/enforcement/case-summary-settlement-formosa-plastics-corporation-site-wide-corrective-actions-point.
EPA, 2017. IRIS toxicological review of benzo[a]pyrene (final report)|IRIS|US EPA. https://cfpub.epa.gov/ncea/iris_drafts/recordisplay.cfm?deid=329750.
FDA, 2010. Protocol for interpretation and use of sensory testing and analytical chemistry results for re-opening oil-impacted areas closed to seafood harvesting due to the Deepwater Horizon oil spill, FDA. https://www.fda.gov/food/food-safety-during-emergencies/protocol-interpretation-and-use-sensory-testing-and-analytical-chemistry-results-re-opening-oil.
Fears, D., 2018. A 14-year-long oil spill in the Gulf of Mexico verges on becoming one of the worst in US history. Wash. Post 21.
Finklea, B., Miller, G., Busbee, D., 2000. Polychlorinated biphenyl residues in blubber of male Atlantic bottlenose dolphins (Tursiops truncatus) that stranded and died at Matagorda Bay. Bull. Environ. Contam. Toxicol. 64 (3), 323–332.
Fisher, W.S., Oliver, L.M., Winstead, J.T., Long, E.R., 2000. A survey of oysters Crassostrea virginica from Tampa Bay, Florida: associations of internal defense measurements with contaminant burdens. Aquat. Toxicol. 51 (1), 115–138.
Frank, D.S., Mora, M.A., Sericano, J.L., Blankenship, A.L., Kannan, K., Giesy, J.P., 2001. Persistent organochlorine pollutants in eggs of colonial waterbirds from Galveston Bay and East Texas, USA. Environmental Toxicology and Chemistry: An International Journal 20 (3), 608–617.
Gavrilescu, M., Demnerová, K., Aamand, J., Agathos, S., Fava, F., 2015. Emerging pollutants in the environment: present and future challenges in biomonitoring, ecological risks and bioremediation. New Biotechnol. 32 (1), 147–156. https://doi.org/10.1016/j.nbt.2014.01.001 (2015/01/25).
Geissen, V., Mol, H., Klumpp, E., Umlauf, G., Nadal, M., van der Ploeg, M., van de Zee, S. E.A.T.M., Ritsema, C.J., 2015. Emerging pollutants in the environment: a challenge for water resource management. International Soil and Water Conservation Research 3 (1), 57–65. https://doi.org/10.1016/j.iswcr.2015.03.002 (2015/03/01).
Giesy, J.P., Kannan, K., 1998. Dioxin-like and non-dioxin-like toxic effects of polychlorinated biphenyls (PCBs): implications for risk assessment. Crit. Rev. Toxicol. 28 (6), 511–569.
Goldberg, E.D., Bowen, V.T., Farrington, J.W., Harvey, G., Martin, J.H., Parker, P.L., Risebrough, R.W., Robertson, W., Schneider, E., Gamble, E., 1978. The mussel watch. Environ. Conserv. 5 (2), 101–125.
Gómara, B., Bordajandi, L.R., Fernández, M.A., Herrero, L., Abad, E., Ábalos, M., Rivera, J., González, M.J.é., 2005. Levels and trends of polychlorinated dibenzo-p-dioxins/furans (PCDD/Fs) and dioxin-like polychlorinated biphenyls (PCBs) in Spanish commercial fish and shellfish products, 1995–2003. J. Agric. Food Chem. 53 (21), 8406–8413.
Guidetti, G.P., Rigosi, G.L., Marzola, R., 1996. The use of polypropylene in pipeline coatings. Prog. Org. Coat. 27 (1), 79–85. https://doi.org/10.1016/0300-9440(95)00523-4 (1996/01/01).
HARC, 2014. Oil spills - a continual risk for Galveston Bay, Houston Advanced Research Center (HARC). https://www.harcresearch.org/features/Oils_Spills_a%20_Continual_Risk_for_Galveston_Bay_Habitats.
Hays, K., 2019. Formosa Plastics' Texas polyethylene plant operational, second plant to come online in December, S&P Global. https://www.spglobal.com/commodityinsights/en/market-insights/latest-news/chemicals/112619-formosa-plastics-texas-polyethylene-plant-operational-second-plant-to-come-online-in-december.
Hernout, B., Leleux, J., Lynch, J., Ramaswamy, K., Faulkner, P., Matich, P., Hala, D., 2020. The integration of fatty acid biomarkers of trophic ecology with pollutant body-burdens of PAHs and PCBs in four species of fish from Sabine Lake, Texas. Environmental Advances 1, 100001. https://doi.org/10.1016/j.envadv.2020.100001 (2020/09/01).
Honda, M., Suzuki, N., 2020. Toxicities of polycyclic aromatic hydrocarbons for aquatic animals. Int. J. Environ. Res. Public Health 17 (4), 1363.
Hong, J., Kima, H.Y., Kim, D.G., Seo, J., Kimb, K.J., 2004. Rapid determination of chlorinated pesticides in fish by freezing-lipid filtration, solid-phase extraction and gas chromatography-mass spectrometry. J. Chromatogr. A 1038 (1–2), 27–35. https://doi.org/10.1016/j.chroma.2004.03.003 (Jun 4).
Horton, A.A., Walton, A., Spurgeon, D.J., Lahive, E., Svendsen, C., 2017. Microplastics in freshwater and terrestrial environments: evaluating the current understanding to identify the knowledge gaps and future research priorities. Sci. Total Environ. 586, 127–141. https://doi.org/10.1016/j.scitotenv.2017.01.190 (2017/05/15).
Hossain, M.T., Shahid, M.A., Mahmud, N., Habib, A., Rana, M.M., Khan, S.A., Hossain, M.D., 2024. Research and application of polypropylene: a review. Discover Nano 19 (1), 2.
Jafarabadi, A.R., Bakhtiari, A.R., Yaghoobi, Z., Yap, C.K., Maisano, M., Cappello, T., 2019. Distributions and compositional patterns of polycyclic aromatic hydrocarbons (PAHs) and their derivatives in three edible fishes from Kharg coral Island, Persian Gulf, Iran. Chemosphere 215, 835–845.
Jesus, F., Pereira, J.L., Campos, I., Santos, M., Ré, A., Keizer, J., Nogueira, A., Gonçalves, F.J., Abrantes, N., Serpa, D., 2022. A review on polycyclic aromatic hydrocarbons distribution in freshwater ecosystems and their toxicity to benthic fauna. Sci. Total Environ. 820, 153282.
Johnson, W., Kimbrough, K., Lauenstein, G., Christensen, J., 2009. Chemical contamination assessment of Gulf of Mexico oysters in response to hurricanes Katrina and Rita. Environ. Monit. Assess. 150, 211–225.
Kanhai, L.D.K., Gobin, J.F., Beckles, D.M., Lauckner, B., Mohammed, A., 2015. Polycyclic aromatic hydrocarbons (PAHs) in Crassostrea rhizophorae and Cathorops spixii from the Caroni Swamp, Trinidad, West Indies. Environ. Sci. Pollut. Res. 22, 1366–1379.
Kannan, K., Blankenship, A., Jones, P., Giesy, J., 2000. Toxicity reference values for the toxic effects of polychlorinated biphenyls to aquatic mammals. Hum. Ecol. Risk. Assess. 6 (1), 181–201.
Kennicutt, M.C., 2017. Sediment contaminants of the Gulf of Mexico. In: Ward, C.H. (Ed.), Habitats and Biota of the Gulf of Mexico: Before the Deepwater Horizon Oil Spill: Volume 1: Water Quality, Sediments, Sediment Contaminants, Oil and Gas Seeps, Coastal Habitats, Offshore Plankton and Benthos, and Shellfish. Springer New York, pp. 217–273. https://doi.org/10.1007/978-1-4939-3447-8_4.
Lee, B.M., Shim, G.A., 2007. Dietary exposure estimation of benzo [a] pyrene and cancer risk assessment. J. Toxicol. Environ. Health A 70 (15–16), 1391–1394.
Leslie, H.A., van Velzen, M.J.M., Brandsma, S.H., Vethaak, A.D., Garcia-Vallejo, J.J., Lamoree, M.H., 2022. Discovery and quantification of plastic particle pollution in human blood. Environ. Int. 163, 107199. https://doi.org/10.1016/j.envint.2022.107199 (May).
Lim, K.P., Lim, P.E., Yusoff, S., Sun, C., Ding, J., Loh, K.H., 2022. A meta-analysis of the characterisations of plastic ingested by fish globally. Toxics 10 (4), 186.
Lipiatou, E., Saliot, A., 1991. Fluxes and transport of anthropogenic and natural polycyclic aromatic hydrocarbons in the western Mediterranean Sea. Mar. Chem. 32 (1), 51–71.
Liu, Z., Liu, J., Zhu, Q., Wu, W., 2012. The weathering of oil after the Deepwater Horizon oil spill: insights from the chemical composition of the oil from the sea surface, salt marshes and sediments. Environ. Res. Lett. 7 (3), 035302.
Lloyd, J., Lu, K., Liu, Z., 2024. Investigating concentrations and sources of polycyclic aromatic hydrocarbons in South and Central Texas bays and estuaries along the Gulf of Mexico, USA. Front. Mar. Sci. 11, 1456717.
Maddah, H.A., 2016. Polypropylene as a promising plastic: a review. Am. J. Polym. Sci 6 (1), 1–11.
Mintenig, S., Bäuerlein, P.S., Koelmans, A.A., Dekker, S.C., Van Wezel, A., 2018. Closing the gap between small and smaller: towards a framework to analyse nano-and microplastics in aqueous environmental samples. Environ. Sci. Nano 5 (7), 1640–1649.
Monosson, E., Ashley, J., McElroy, A., Woltering, D., Elskus, A., 2003. PCB congener distributions in muscle, liver and gonad of Fundulus heteroclitus from the lower Hudson River Estuary and Newark Bay. Chemosphere 52 (4), 777–787.
Montuori, P., De Rosa, E., Di Duca, F., De Simone, B., Scippa, S., Russo, I., Sarnacchiaro, P., Triassi, M., 2022. Polycyclic Aromatic Hydrocarbons (PAHs) in the dissolved phase, particulate matter, and sediment of the Sele River, Southern Italy: a focus on distribution, risk assessment, and sources. Toxics 10 (7), 401.
Moon, H.-B., Ok, G., 2006. Dietary intake of PCDDs, PCDFs and dioxin-like PCBs, due to the consumption of various marine organisms from Korea. Chemosphere 62 (7), 1142–1152.
Moore-Eissenberg, L., 2019. No more nurdles? Formosa's agreement to stop pumping plastics into Lavaca Bay is historic, Texas Monthly. https://www.texasmonthly.com/news-politics/nurdles-formosas-agreement-stop-plastics-lavaca-bay-historic/.
Murawski, S.A., Hogarth, W.T., Peebles, E.B., Barbeiri, L., 2014. Prevalence of external skin lesions and polycyclic aromatic hydrocarbon concentrations in Gulf of Mexico fishes, post-Deepwater Horizon. Trans. Am. Fish. Soc. 143 (4), 1084–1097.
Neff, J., Cox, B.A., Dixit, D., Anderson, J., 1976. Accumulation and release of petroleum-derived aromatic hydrocarbons by four species of marine animals. Mar. Biol. 38, 279–289.
NOAA, 2020. Water cleaning capacity of oysters could mean extra income for Chesapeake Bay growers, NCCOS Coastal Science Website. https://coastalscience.noaa.gov/news/water-cleaning-capacity-of-oysters-could-mean-extra-income-for-chesapeake-bay-growers-video/.
NOAA, 2024. Gulf of Mexico data atlas - oil and gas structures. https://www.ncei.noaa.gov/maps/gulf-data-atlas/atlas.htm?plate=Offshore%20Structures. (Accessed 17 January 2024).
Nolen, R.M., Faulkner, P., Ross, A.D., Kaiser, K., Quigg, A., Hala, D., 2022. PFASs pollution in Galveston Bay surface waters and biota (shellfish and fish) following AFFFs use during the ITC fire at Deer Park (March 17th–20th 2019), Houston, TX. Sci. Total Environ. 805, 150361.
Olayinka, O.O., Adewusi, A.A., Olujimi, O.O., Aladesida, A.A., 2019. Polycyclic aromatic hydrocarbons in sediment and health risk of fish, crab and shrimp around Atlas Cove, Nigeria. Journal of Health and Pollution 9 (24), 191204.
OSHA, 2005. Five employees killed in explosion; four injured. https://www.osha.gov/ords/imis/accidentsearch.accident_detail?id=200271294.
OSPAR, 2018. OSPAR Background Document on Pre-production Plastic Pellets, pp. 1–35. https://www.ospar.org/documents?v=39764. (Accessed 13 January 2025).
Oziolor, E.M., Apell, J.N., Winfield, Z.C., Back, J.A., Usenko, S., Matson, C.W., 2018. Polychlorinated biphenyl (PCB) contamination in Galveston Bay, Texas: comparing concentrations and profiles in sediments, passive samplers, and fish. Environ. Pollut. 236, 609–618. https://doi.org/10.1016/j.envpol.2018.01.086 (May).
Ozougwu, J.C., 2017. Physiology of the liver. International Journal of Research in Pharmacy and Biosciences 4 (8), 13–24.
Patel, A.B., Shaikh, S., Jain, K.R., Desai, C., Madamwar, D., 2020. Polycyclic aromatic hydrocarbons: sources, toxicity, and remediation approaches. Front. Microbiol. 11, 562813.
Peng, X., Chen, G., Fan, Y., Zhu, Z., Guo, S., Zhou, J., Tan, J., 2021. Lifetime bioaccumulation, gender difference, tissue distribution, and parental transfer of organophosphorus plastic additives in freshwater fish. Environ. Pollut. 280, 116948. https://doi.org/10.1016/j.envpol.2021.116948 (2021/07/01).
Pulster, E.L., Gracia, A., Armenteros, M., Toro-Farmer, G., Snyder, S.M., Carr, B.E., Schwaab, M.R., Nicholson, T.J., Mrowicki, J., Murawski, S.A., 2020. A first

comprehensive baseline of hydrocarbon pollution in Gulf of Mexico fishes. Sci. Rep. 10 (1), 6437. https://doi.org/10.1038/s41598-020-62944-6 (2020/04/15).
R, 2024. R: a language and environment for statistical computing, R Foundation for Statistical Computing. https://www.R-project.org/.
Ramseur, J.L., 2010. Deepwater Horizon Oil Spill: The Fate of the Oil.
Rauert, C., Pan, Y., Okoffo, E.D., O'Brien, J.W., Thomas, K.V., 2022. Extraction and Pyrolysis-GC-MS analysis of polyethylene in samples with medium to high lipid content. Journal of Environmental Exposure Assessment 1 (2), 13.
Ribeiro, F., Okoffo, E.D., O'Brien, J.W., Fraissinet-Tachet, S., O'Brien, S., Gallen, M., Samanipour, S., Kaserzon, S., Mueller, J.F., Galloway, T., 2020. Quantitative analysis of selected plastics in high-commercial-value Australian seafood by pyrolysis gas chromatography mass spectrometry. Environ. Sci. Technol. 54 (15), 9408–9417.
Ribeiro, F., Okoffo, E.D., O'Brien, J.W., O'Brien, S., Harris, J.M., Samanipour, S., Kaserzon, S., Mueller, J.F., Galloway, T., Thomas, K.V., 2021. Out of sight but not out of mind: size fractionation of plastics bioaccumulated by field deployed oysters. Journal of Hazardous Materials Letters 2, 100021.
Rice, J., 2019. Texas A&M water researchers find waxy residue near deer park disaster, Houston Public Media. https://www.houstonpublicmedia.org/articles/news/2019/03/28/327062/texas-am-water-researchers-found-waxy-residue-near-deer-park-disaster/.
Robinson, L., Campbell, P., Butler, L., 1996. Trends in commercial fishery landings, 1972–1995. In: Management Data Series, No. 127. Texas Parks and Wildlife Department Coastal Fisheries Division, Austin, Texas.
Romero, I.C., Chanton, J.P., Brooks, G.R., Bosman, S., Larson, R.A., Harris, A., Schwing, P., Diercks, A., 2021. Molecular markers of biogenic and oil-derived hydrocarbons in deep-sea sediments following the Deepwater Horizon spill. Front. Mar. Sci. 8, 637970.
Ronca, S., 2017. Chapter 10 - polyethylene. In: Gilbert, M. (Ed.), Brydson's Plastics Materials, Eighth edition. Butterworth-Heinemann, pp. 247–278. https://doi.org/10.1016/B978-0-323-35824-8.00010-4.
Ropicki, A.H., Dudensing, R.C., Rhonda Balboa, B., 2016. The Economic Impacts of Recreational Fishing in the Matagorda Bay System.
Rotkin-Ellman, M., Wong, K.K., Solomon, G.M., 2012. Seafood contamination after the BP Gulf oil spill and risks to vulnerable populations: a critique of the FDA risk assessment. Environ. Health Perspect. 120 (2), 157–161.
Rowe, G.T., Fernando, H., Elferink, C., Ansari, G.A.S., Sullivan, J., Heathman, T., Quigg, A., Petronella Croisant, S., Wade, T.L., Santschi, P.H., 2020. Polycyclic aromatic hydrocarbons (PAHs) cycling and fates in Galveston Bay, Texas, USA. PLoS One 15 (12), e0243734. https://doi.org/10.1371/journal.pone.0243734.
Safe, S.H., 1994. Polychlorinated biphenyls (PCBs): environmental impact, biochemical and toxic responses, and implications for risk assessment. Crit. Rev. Toxicol. 24 (2), 87–149.
Safe, S., Hutzinger, O., 1984. Polychlorinated biphenyls (PCBs) and polybrominated biphenyls (PBBs): biochemistry, toxicology, and mechanism of action. CRC Crit. Rev. Toxicol. 13 (4), 319–395.
Safe, Bandiera, S., Sawyer, T., Robertson, L., Safe, L., Parkinson, A., Thomas, P.E., Ryan, D.E., Reik, L.M., Levin, W., 1985. PCBs: structure–function relationships and mechanism of action. Environ. Health Perspect. 60, 47–56.
Santos, L., Miranda, D., Hatje, V., Albergaria-Barbosa, A., Leonel, J., 2020. PCBs occurrence in marine bivalves and fish from Todos os Santos Bay, Bahia, Brazil. Mar. Pollut. Bull. 154, 111070.
Savas, L.A., Tayfun, U., Dogan, M., 2016. The use of polyethylene copolymers as compatibilizers in carbon fiber reinforced high density polyethylene composites. Compos. Part B Eng. 99, 188–195. https://doi.org/10.1016/j.compositesb.2016.06.043 (2016/08/15).
Senathirajah, K., Attwood, S., Bhagwat, G., Carbery, M., Wilson, S., Palanisami, T., 2021. Estimation of the mass of microplastics ingested–a pivotal first step towards human health risk assessment. J. Hazard. Mater. 404, 124004.
Shakiba, M., Rezvani Ghomi, E., Khosravi, F., Jouybar, S., Bigham, A., Zare, M., Abdouss, M., Moaref, R., Ramakrishna, S., 2021. Nylon—a material introduction and overview for biomedical applications. Polym. Adv. Technol. 32 (9), 3368–3383.
Simoneit, B.R., 1985. Application of molecular marker analysis to vehicular exhaust for source reconciliations. Int. J. Environ. Anal. Chem. 22 (3–4), 203–232.
Snyder, S.M., Pulster, E.L., Wetzel, D.L., Murawski, S.A., 2015. PAH exposure in Gulf of Mexico demersal fishes, post-Deepwater Horizon. Environ. Sci. Technol. 49 (14), 8786–8795.
Solo-Gabriele, H.M., Fiddaman, T., Mauritzen, C., Ainsworth, C., Abramson, D.M., Berenshtein, I., Chassignet, E.P., Chen, S.S., Conmy, R.N., Court, C.D., Dewar, W.K., Farrington, J.W., Feldman, M.G., Ferguson, A.C., Fetherston-Resch, E., French-McCay, D., Hale, C., He, R., Kourafalou, V.H., Lee, K., Liu, Y., Masi, M., Maung-Douglass, E.S., Morey, S.L., Murawski, S.A., Paris, C.B., Perlin, N., Pulster, E.L., Quigg, A., Reed, D.J., Ruzicka, J.J., Sandifer, P.A., Shepherd, J.G., Singer, B.H., Stukel, M.R., Sutton, T.T., Weisberg, R.H., Wiesenburg, D., Wilson, C.A., Wilson, M., Wowk, K.M., Yanoff, C., Yoskowitz, D., 2021. Towards integrated modeling of the long-term impacts of oil spills. Mar. Policy 131, 104554. https://doi.org/10.1016/j.marpol.2021.104554 (2021/09/01).
Stafford, G.D., Huggett, R., MacGregor, A.R., Graham, J., 1986. The use of nylon as a denture-base material. J. Dent. 14 (1), 18–22. https://doi.org/10.1016/0300-5712(86)90097-7 (1986/02/01).
Steevens, J.A., Reiss, M.R., Pawlisz, A.V., 2005. A methodology for deriving tissue residue benchmarks for aquatic biota: a case study for fish exposed to 2, 3, 7, 8-tetrachlorodibenzo-p-dioxin and equivalents. Integrated Environmental Assessment and Management: An International Journal 1 (2), 142–151.
Sui, Q., Yang, X., Sun, X., Zhu, L., Zhao, X., Feng, Z., Xia, B., Qu, K., 2024. Bioaccumulation of polycyclic aromatic hydrocarbons and their human health risks depend on the characteristics of microplastics in marine organisms of Sanggou Bay, China. J. Hazard. Mater. 473, 134622.
Sverdrup, L.E., Nielsen, T., Krogh, P.H., 2002. Soil ecotoxicity of polycyclic aromatic hydrocarbons in relation to soil sorption, lipophilicity, and water solubility. Environ. Sci. Technol. 36 (11), 2429–2435.
TDT, 2020. Texas Port profiles, Texas Department of Transportation. https://ftp.dot.state.tx.us/pub/txdot-info/mrt/port-profiles.pdf.
Tiedje, J.M., Quensen, J.F., Chee-Sanford, J., Schimel, J.P., Boyd, S.A., 1993. Microbial reductive dechlorination of PCBs. Biodegradation 4, 231–240.
Tobiszewski, M., Namieśnik, J., 2012. PAH diagnostic ratios for the identification of pollution emission sources. Environ. Pollut. 162, 110–119.
Tresaugue, M., 2014. Oil spill befouls Matagorda Island, Houston Chronicle. https://www.houstonchronicle.com/news/houston-texas/houston/article/oil-spill-befouls-matagorda-island-5355482.php.
Trevisan, R., Flores-Nunes, F., Dolores, E.S., Mattos, J.J., Piazza, C.E., Sasaki, S.T., Taniguchi, S., Montone, R.C., Bícego, M.C., Dos Reis, I.M., 2017. Thiol oxidation of hemolymph proteins in oysters Crassostrea brasiliana as markers of oxidative damage induced by urban sewage exposure. Environ. Toxicol. Chem. 36 (7), 1833–1845.
Trevizo, P., 2019. Hundreds of dead fish, crabs seen on Kemah property after ship channel spill, Houston Chronicle. https://www.houstonchronicle.com/news/houston-texas/houston/article/Hundreds-of-dead-fish-crabs-seen-on-Kemah-13841902.php.
TSHA, 2023. Handbook of Texas. https://www.tshaonline.org/handbook.
Van den Berg, M., Birnbaum, L., Bosveld, A., Brunström, B., Cook, P., Feeley, M., Giesy, J.P., Hanberg, A., Hasegawa, R., Kennedy, S.W., 1998. Toxic equivalency factors (TEFs) for PCBs, PCDDs, PCDFs for humans and wildlife. Environ. Health Perspect. 106 (12), 775–792.
Vandermeulen, J., 1987. Toxicity and sublethal effects of petroleum hydrocarbons in freshwater biota. In: Oil in Freshwater: Chemistry, Biology, Countermeasure Technology, pp. 267–303.
Vega, R.R., Neill, W.H., Gold, J.R., Ray, M.S., 2011. Enhancement of Texas sciaenids (red drum and spotted seatrout). In: NOAA Technical Memorandum NMFS-F/SPO-113, pp. 85–92.
Vidal-Liñán, L., Bellas, J., Soriano, J.A., Concha-Graña, E., Muniategui, S., Beiras, R., 2016. Bioaccumulation of PCB-153 and effects on molecular biomarkers acetylcholinesterase, glutathione-S-transferase and glutathione peroxidase in Mytilus galloprovincialis mussels. Environ. Pollut. 214, 885–891. https://doi.org/10.1016/j.envpol.2016.04.083 (2016/07/01).
von Friesen, L.W., Granberg, M.E., Hassellöv, M., Gabrielsen, G.W., Magnusson, K., 2019. An efficient and gentle enzymatic digestion protocol for the extraction of microplastics from bivalve tissue. Mar. Pollut. Bull. 142, 129–134.
Wang, H., Huang, W., Gong, Y., Chen, C., Zhang, T., Diao, X., 2020. Occurrence and potential health risks assessment of polycyclic aromatic hydrocarbons (PAHs) in different tissues of bivalves from Hainan Island, China. Food Chem. Toxicol. 136, 111108.
Warren, C.J., MacFadyen, A., Henry Jr., C., 2014. Mapping oil for the destroyed Taylor Energy Site in the Gulf of Mexico. In: International Oil Spill Conference Proceedings.
Williams, A.K., Bacosa, H.P., Quigg, A., 2017. The impact of dissolved inorganic nitrogen and phosphorous on responses of microbial plankton to the Texas City "Y" oil spill in Galveston Bay, Texas (USA). Mar. Pollut. Bull. 121 (1–2), 32–44.
Wilson, D., 2018. Report shows plastic pollution a threat to Texas Gulf Coast. Waterkeeper Alliance. https://waterkeeper.org/news/report-shows-plastic-pollution-a-threat-to-texas-gulf-coast/ (Accessed March 2025).
Wisse, E., De Zanger, R., Charels, K., Van Der Smissen, P., McCuskey, R., 1985. The liver sieve: considerations concerning the structure and function of endothelial fenestrae, the sinusoidal wall and the space of Disse. Hepatology 5 (4), 683–692.
Wolska, L., Mechlińska, A., Rogowska, J., Namieśnik, J., 2012. Sources and fate of PAHs and PCBs in the marine environment. Crit. Rev. Environ. Sci. Technol. 42 (11), 1172–1189.
Wood, N.J., 2014. The liver as a firewall—clearance of commensal bacteria that have escaped from the gut. Nat. Rev. Gastroenterol. Hepatol. 11 (7), 391.
Xiang, Y., Xing, Z., Liu, J., Qin, W., Huang, X., 2020. Recent advances in the biodegradation of polychlorinated biphenyls. World J. Microbiol. Biotechnol. 36, 1–10.
Xu, F.-L., Wu, W.-J., Wang, J.-J., Qin, N., Wang, Y., He, Q.-S., He, W., Tao, S., 2011. Residual levels and health risk of polycyclic aromatic hydrocarbons in freshwater fishes from Lake Small Bai-Yang-Dian, Northern China. Ecol. Model. 222 (2), 275–286.
Yeager, K.M., Santschi, P.H., Rifai, H.S., Suarez, M.P., Brinkmeyer, R., Hung, C.-C., Schindler, K.J., Andres, M.J., Weaver, E.A., 2007. Dioxin chronology and fluxes in sediments of the Houston Ship Channel, Texas: influences of non-steady-state sediment transport and total organic carbon. Environ. Sci. Technol. 41 (15), 5291–5298.
Yunker, M.B., Snowdon, L.R., Macdonald, R.W., Smith, J.N., Fowler, M.G., Skibo, D.N., McLaughlin, F.A., Danyushevskaya, A., Petrova, V., Ivanov, G., 1996. Polycyclic aromatic hydrocarbon composition and potential sources for sediment samples from the Beaufort and Barents Seas. Environ. Sci. Technol. 30 (4), 1310–1320.
Yunker, M.B., Macdonald, R.W., Goyette, D., Paton, D.W., Fowler, B.R., Sullivan, D., Boyd, J., 1999. Natural and anthropogenic inputs of hydrocarbons to the Strait of Georgia. Sci. Total Environ. 225 (3), 181–209. https://doi.org/10.1016/S0048-9697(98)00362-3 (1999/01/26).
Zhang, X., Cheng, S., Huang, X., Logan, B.E., 2010. The use of nylon and glass fiber filter separators with different pore sizes in air-cathode single-chamber microbial fuel cells. Energy Environ. Sci. 3 (5), 659–664.

Zhang, J., Wang, L., Trasande, L., Kannan, K., 2021. Occurrence of polyethylene terephthalate and polycarbonate microplastics in infant and adult feces. Environ. Sci. Technol. Lett. 8 (11), 989–994. https://doi.org/10.1021/acs.estlett.1c00559 (2021/11/09).

Zhao, Z., Zhang, L., Cai, Y., Chen, Y., 2014. Distribution of polycyclic aromatic hydrocarbon (PAH) residues in several tissues of edible fishes from the largest freshwater lake in China, Poyang Lake, and associated human health risk assessment. Ecotoxicol. Environ. Saf. 104, 323–331. https://doi.org/10.1016/j.ecoenv.2014.01.037 (Jun).

Zitouni, N., Bousserrhine, N., Missawi, O., Boughattas, I., Chèvre, N., Santos, R., Belbekhouche, S., Alphonse, V., Tisserand, F., Balmassiere, L., 2021. Uptake, tissue distribution and toxicological effects of environmental microplastics in early juvenile fish Dicentrarchus labrax. J. Hazard. Mater. 403, 124055.